Variations in the chemical composition of the submicron aerosol and in the sources of the organic fraction at a regional background site of the Po Valley (Italy)

M. Bressi[1], F. Cavalli[1], C. A. Belis[1], J. -P. Putaud[1], R. Fröhlich[2], S. Martins dos Santos[1], E. Petralia[3], A. S. H. Prévôt[2], M. Berico[3], A. Malaguti[3] and F. Canonaco[2]

[1]European Commission, Joint Research Centre, Institute for Environment and Sustainability, Air and Climate Unit, Via Enrico Fermi 2749, Ispra (VA) 21027, Italy.

[2]Paul Scherrer Institute, Laboratory of Atmospheric Chemistry, Villigen 5232, Switzerland.

[3]Italian National Agency for New Technologies, Energy and Sustainable Economic Development (ENEA), Via Martiri di Monte Sole 4, Bologna 40129, Italy.

Correspondence to:

michael.s.bressi@gmail.com, claudio.belis@jrc.ec.europa.eu, fabrizia.cavalli@jrc.ec.europa.eu

Abstract

Fine particulate matter (PM) levels and resulting impacts on human health are in the Po Valley (Italy) among the highest in Europe. To build effective PM abatement strategies, it is necessary to characterize fine PM chemical composition, sources and atmospheric processes on long time scales (>months), with short time resolution (<day), and with particular emphasis on the predominant organic fraction. Although previous studies have been conducted in this region, none of them addressed all these aspects together. For the first time in the Po Valley, we investigate the chemical composition of non-refractory submicron PM (NR-PM$_1$) with a time-resolution of 30 minutes at the regional background site of Ispra during one full year, using an Aerosol Chemical Speciation Monitor (ACSM) under the most up-to-date and stringent quality assurance protocol. The identification of the main components of the organic fraction is made using the Multilinear-Engine 2 algorithm implemented within the latest version of the SoFi toolkit. In addition, with a view of a potential implementation of ACSM measurements in European air quality networks as a replacement of traditional filter-based techniques, parallel multiple off-line analyses were carried out to assess the performance of the ACSM in the determination of PM chemical species regulated by Air Quality Directives. The annual NR-PM$_1$ level monitored at the study site (14.2 μg/m^3) is among the

32 highest in Europe, and is even comparable to levels reported in urban areas like New York City and Tokyo.

33 On the annual basis, submicron particles are primarily composed of organic aerosol (OA, 58% of NR-PM$_1$).

34 This fraction was apportioned into oxygenated OA (OOA, 66%), hydrocarbon-like OA (HOA, 11% of OA),

35 and biomass burning OA (BBOA, 23%). Among the primary sources of OA, biomass burning (23%) is thus

36 bigger than fossil fuel combustion (11%). Significant contributions of aged secondary organic aerosol

37 (OOA) are observed throughout the year. The unexpectedly high degree of oxygenation estimated during

38 wintertime is probably due to the contribution of secondary BBOA and the enhancement of aqueous

39 phase production of OOA during cold months. BBOA and nitrate are the only components of which

40 contributions increase with the NR-PM$_1$ levels. Therefore, biomass burning and NO$_x$ emission reductions

41 would be particularly efficient in limiting submicron aerosol pollution events. Abatement strategies

42 conducted during cold seasons appear to be more efficient than annual-based policies. In a broader

43 context, further studies using high-time resolution analytical techniques on a long-term basis for the

44 characterization of fine aerosol should help better shape our future air quality policies, which constantly

45 need refinement.

46

47   1. Introduction

48 The Po Valley region - located in northern Italy - is amongst the most polluted areas in Europe (van

49 Donkelaar et al., 2010; EEA, 2013). Annual PM$_{2.5}$ (particulate matter with an aerodynamic diameter below

50 2.5 μm) mean concentrations can significantly exceed the European PM$_{2.5}$ annual limit value (25 μg/m^3 in

51 2015, European Directive 2008/50/EC) and the recommendations of the World Health Organization (PM$_{2.5}$

52 annual average of 10 μg/m^3; WHO, 2006) at urban (e.g. Bologna, 35.8 μg/m^3) and regional background

53 sites (e.g. Ispra, 32.2 μg/m^3; Putaud et al., 2010). Consequently, PM$_{2.5}$ impacts on human health are among

54 the most severe in Europe (EC, 2005), while impacts on the local radiative forcing are substantial (Clerici

55 and Mélin, 2008; Ferrero et al., 2014; Putaud et al., 2014b). Effective PM abatement strategies are thus

56 needed in the Po Valley and require an in-depth knowledge of the chemical composition of fine PM, to

57 quantify its sources and the atmospheric processes leading to its secondary formation.

58   In this region, high levels of fine aerosol are mostly due to the conjunction of i) high pollutant

59 emissions related to industrial, transport, biomass burning and agricultural activities - the Po river basin

60 hosting 37% of the Italian industries, 55% of the livestock and contributing 35% of the Italian agricultural

61 production (WMO et al., 2012) - and ii) the specific geography and topography of this area - a flat basin

62 surrounded by the Alps and Apennine Mountains dominated by weak winds that favour the accumulation

63 of pollutants (Decesari et al., 2014; Kukkonen et al., 2005; Pernigotti et al., 2012). As a consequence, PM

64 levels are not only high in urban areas but also at regional and rural background sites, which are key
65 locations for investigating air pollution due to their distance from local sources and local phenomena.
66 Measurements of fine PM mass and chemical composition at rural background sites are in addition
67 specifically required in the current European Directive on air quality (EU, 2008).

68 Previous studies have investigated the properties of fine aerosols at regional and rural background
69 sites of the Po valley region, including their chemical characteristics (e.g. Carbone et al., 2014; Putaud et
70 al., 2002, 2010; Saarikoski et al., 2012), and their main sources (Belis et al., 2013; Gilardoni et al., 2011;
71 Larsen et al., 2012; Perrone et al., 2012). Fine aerosols are primarily made of organics (30-80% of fine PM
72 mass, depending on the site and season studied), followed by ammonium nitrate and ammonium sulfate.
73 Their main sources are fossil fuel, biomass burning and biogenic emissions to name a few. In addition,
74 studies based on aerosol mass spectrometer measurements have been conducted in the Po valley, with
75 the aim of characterizing specific phenomena (e.g. fog events, cooking aerosols) or seasons (Dall'Osto et
76 al., 2015; Decesari et al., 2014; Gilardoni et al., 2014; Saarikoski et al., 2012). In studies dealing with long
77 time-series (entire season or year), the chemical composition of fine aerosol is generally measured with a
78 relatively low time resolution (typically 24 hours), thus preventing from studying its diurnal variation and
79 short-lived chemical-physical processes. When documented with higher time-resolutions (1 hour or less),
80 aerosol chemical composition and its sources are usually characterized for intensive campaigns of a few
81 weeks only, hence not suitable to depict the seasonal or yearly air quality situation. In addition, the
82 complexity of the fine organic fraction (e.g. Jimenez et al., 2009) requires state-of-the-art analytical and
83 source apportionment (SA) techniques to identify organic aerosol chemical properties and sources.

84 The recently developed Aerosol Chemical Speciation Monitor (ACSM, Aerodyne Research Inc., Ng
85 et al., 2011a) is suitable to fill these gaps by providing the chemical composition of non-refractory
86 submicron aerosols (NR-PM$_1$) with a time resolution of 30 min, while operating on long time scales. Even
87 though promising results have been recently reported (e.g. Budisulistiorini et al., 2014; Canonaco et al.,
88 2013, 2015; Minguillón et al., 2015; Ng et al., 2011a; Petit et al., 2015; Ripoll et al., 2015; Sun et al., 2012),
89 this technique is still novel and requires additional field deployment to test its consistency with
90 independent methods for the monitoring of fine PM chemistry (e.g. filter measurements). In addition,
91 information on the accuracy of this technique is of paramount importance given the growing number of
92 ACSMs in Europe and the necessity to build a network of quality assured and harmonized instruments for
93 comparability of results – at present about 20 ACSMs are in operation in Europe (http://www.psi.ch/acsm-
94 stations/overview-full-period) within the frame of the EU ACTRIS network (Aerosols, Clouds, and Traces
95 gases Research InfraStructure, http://www.actris.eu/). Moreover, by using receptor models, the

96   apportionment of organic aerosol (OA) into its major components - hydrocarbon-like (HOA), biomass

97   burning (BBOA) and oxygenated OA (OOA) - can be performed (Lanz et al., 2007; Zhang et al., 2011 and

98   references therein).

99   In this study, we used an ACSM during one year with a 30-min time-resolution at a regional

100   background site of the Po Valley and performed subsequent SA analyses with the aim of: i) describing the

101   high time resolved chemical composition of NR-PM$_1$ on a long time-scale, to better understand the

102   physicochemical processes driving its temporal variations, ii) apportioning the organic fraction into its

103   main sources, iii) identifying PM abatement strategies to efficiently reduce NR-PM$_1$ pollution events at

104   regional background areas of the Po valley, and iv) assessing the atmospheric consistency of ACSM

105   measurements when compared to independent analytical methods, to evaluate its possible

106   implementation in future European Air Quality networks.

107

108   2.   Material and methods

109   2.1. Sampling site

110   Measurements were conducted at the European Commission – Joint Research Centre (EC-JRC) Ispra site

111   (45°48'N, 8°38'E, 217 m a.s.l.; Fig. S1), which is part of the European Monitoring and Evaluation

112   Programme   (EMEP)   measurement   network   (http://www.nilu.no/projects/ccc/

113   sitedescriptions/it/index.html)   and   the   Global   Atmosphere   Watch   (GAW)   regional   stations

114   (http://www.wmo.int/pages/prog/arep/gaw/measurements.html). It is located on the northwest edge of

115   the Po Valley region, 60 km northwest of the Milan urban area. It can be regarded as a "regional/rural

116   background" site following the criteria recommended by the European Environment Agency (Larssen et

117   al., 1999). For simplicity, the term "regional background site" will be used in the following although

118   comparisons with rural background sites from other studies will also be reported. Further information on

119   the study site can be found in Putaud et al. (2014b).

120

121   2.2. Aerosol Chemical Speciation Monitor (ACSM)

122   The recently developed ACSM (Aerodyne Research Inc., ARI) was used to measure the non-refractory (NR)

123   chemical composition (organics, nitrate, sulfate, ammonium, chloride) of submicron particles (PM$_1$) with

124   a 30-min time resolution. The operating principle of the ACSM is similar to the widespread Aerodyne

125   aerosol mass spectrometer (Canagaratna et al., 2007; Jayne et al., 2000), with the difference that the

126   former does not inform on the size distribution of the chemical composition of NR-PM$_1$. A full description

127   of the ACSM can be found in Ng et al. (2011a). Briefly, an aerodynamic lens is used to focus submicron

128 particles (50% transmission range of 75-650 nm; Liu et al., 2007), which are then vaporized in high vacuum,

129 ionized by electron ionization (at 70 eV) and detected by a quadrupole mass spectrometer (Pfeiffer

130 Vacuum Prisma Plus RGA). Two different quadrupole-ACSMs (Q-ACSMs) were used in this study (from

131 March 2013 to February 2014): Q-ACSM#1 from 01 March to 18 August 2013 and Q-ACSM#2 from 20 June

132 2013 to 28 February 2014. Note that Q-ACSM#2 was not running from 3 November to 18 December due

133 to its participation in the first inter-ACSM comparison exercise (Crenn et al., 2015). The reproducibility

134 and consistency with independent measurements are discussed in Sect. 3.1. In the following, orthogonal

135 regressions are reported unless otherwise stated.

136 Both ACSMs were operated with the latest Data Acquisition (DAQ 1.4.3.8 to 1.4.4.5) and Data

137 Analysis (DAS 1.5.3.0 to 1.5.3.2) software (ARI, https://sites.google.com/site/ariacsm/mytemplate-sw)

138 available at the time of use, which are developed within Igor Pro 6.32A (Wavemetrics). Recommendations

139 provided by Aerodyne (2010a, 2010b) and Ng et al. (2011a) were followed for the operation, calibration

140 and data analysis of the ACSMs. Ammonium nitrate calibrations were performed seasonally and used for

141 the determination of experimental nitrate response factors (RF) and ammonium relative ionization

142 efficiencies (RIE, see Sect. S1 for further details). Annual average and season-dependent experimental RF

143 and RIE values were alternatively applied to assess whether the ACSM is stable over multi-seasonal

144 periods (see Sect. 3.1 for results). Seasons are defined as spring (MAM), summer (JJA), autumn (SON) and

145 winter (DJF). RIEs for organics, nitrate and chloride (1.4, 1.1 and 1.3, respectively) were taken from the

146 literature (Canagaratna et al., 2007; Takegawa et al., 2005). RIE for sulfate was experimentally determined

147 based on ammonium sulfate calibrations for ACSM#2, and was taken from the literature for ACSM#1 (see

148 Sect. S1). Collection efficiencies (CE) set as i) a fixed 0.5 value (e.g. Budisulistiorini et al., 2013) or ii)

149 following the composition-dependent CE algorithm introduced by Middlebrook et al. (2012) were

150 compared in order to determine the most appropriate CEs (see Sect. 3.1 for results).

151

152 2.3. Additional analytical techniques

153 Additional measurements routinely performed at the JRC-Ispra site are used in this study (see Putaud et

154 al., 2014a for a full description). $PM_{2.5}$ was sampled on quartz fibre filters (Pall, 2500 QAT-UP) with a

155 Partisol PLUS 2025 sampler equipped with a carbon honeycomb denuder operating at 16.7 L/min from 01

156 March 2013 to 28 February 2014 with daily filter changes at 08:00 UTC. Major ions (NH_4^+, K^+, NO_3^-, SO_4^{2-},

157 etc.) are analysed by ion chromatography (Dionex DX 120 with electrochemical eluent suppression) after

158 extraction in Milli-Q water (Millipore). Organic and elemental carbon (OC and EC, respectively) are

159 quantified by a thermal-optical method (Sunset Dual-optical Lab Thermal-Optical Carbon Aerosol

160   Analyzer) using the EUSAAR-2 protocol (Cavalli et al., 2010). Equivalent black carbon (BC) is measured by

161   a Multi Angle Absorption Photometer (MAAP, Thermo Scientific, model 5012) applying an absorption

162   cross section of 6.6 m^2/g of equivalent black carbon at the operation wavelength of 670 nm. Particle

163   volume concentrations are determined with a home-made Differential Mobility Particle Sizer (DMPS)

164   combining a Vienna-type Differential Mobility Analyser (DMA) and a Condensation Particle Counter (CPC,

165   TSI 3010), following the European Supersites for Atmospheric Aerosol Research (EUSAAR) specifications

166   for DMPS systems (Wiedensohler et al., 2012). Meteorological variables (temperature, pressure, relative

167   humidity, precipitation, wind speed and direction) are determined from a weather transmitter WXT510

168   (Vaisala, Finland). Solar radiation is measured by a CM11 pyranometer (Kipp and Zonen, The Netherlands).

169

170   2.4. Apportionment of the organic fraction

171   The organic fraction was apportioned using the Positive Matrix Factorization approach (PMF, Lanz et al.,

172   2007; Paatero and Tapper, 1994; Ulbrich et al., 2009; Zhang et al., 2011) by applying the Multilinear Engine

173   2 algorithm (ME-2, Paatero, 2000) implemented in the SoFi tool (v4.8, Canonaco et al., 2013; Crippa et al.,

174   2014). Details on the theory and application of PMF and ME-2 can be found in the aforementioned studies.

175   Briefly, PMF aims at factorizing an initial X matrix (representing the temporal variation of *m/z* signals here)

176   into two F and G matrices (representing factor profiles and contributions, respectively) putting a

177   constraint of non-negativity on F and G matrices. Contrary to the classical program used to resolve PMF

178   (e.g. PMF2, PMF3), ME-2 allows any element of the F and G matrices to be constrained with a certain

179   degree of freedom. This ME-2 approach has been typically used to constrain full factor profiles (e.g. Amato

180   et al., 2009; Crippa et al., 2014), specific elemental ratios (e.g. Sturtz et al., 2014) or specific species

181   contribution (e.g. Crawford et al., 2005) in a given factor profile.

182   In our study, ME-2 is applied with and without constraining factor profiles (FPs), using the so-

183   called *a*-value approach (Canonaco et al., 2013) in the former case, which can be described as follows:

184    $(f_{k,j})_{solution}=(f_{k,j})_{reference} \pm a.(f_{k,j})_{reference}$ (1)

185   where k and j are the indexes for the factors and the species, respectively, $f_{k,j}$ is the element (k, j) of the F

186   matrix, the index "solution" stands for the PMF user solution, "reference" for the reference profile and

187   "*a*" is a scalar defined between 0 and 1 (e.g. applying an *a*-value of 0.10 lets ±10% variability to our FP

188   solution with respect to the reference FP). Following Crippa et al. (2014), we perform a sequence of runs

189   with i) unconstrained PMF, ii) fixed HOA, iii) fixed HOA and BBOA, iv) fixed HOA, BBOA and cooking OA

190   (COA) factors before selecting the most appropriate solution. Uncertainties are calculated using the DAS

191   1.5.3.0 version following the methodologies of Allan et al., 2003a and Ulbrich et al. (2009). *m/z* 12 and 13

192 are removed for SA analysis since negative signals are observed most of the time. Reference factor profiles

193 (RFPs) are taken from ambient deconvolved spectra from the Aerosol Mass Spectrometry (AMS) spectral

194 database (Ulbrich et al., 2015). HOA and BBOA profiles are taken from Ng et al. (2011c) (average of profiles

195 from multiple studies) and COA from Crippa et al. (2013). Different a-values are tested (see Sect. 3.2)

196 applying i) relative standard deviations of averaged RFPs defined for every m/z (i.e. assuming that the

197 chosen averaged RFPs are representative of our data set), ii) recommendations of Crippa et al. (2014)

198 based on the SA of 25 European AMS data sets and iii) comparison with independent measurements (e.g.

199 NOx, CO, BC, etc.). Solutions from 2 to 8 factors are investigated in order to choose the appropriate

200 number of factors (see Sect. S2 and 3.2).

201

202   3. Quality assurance / quality control

203   3.1. Quality assurance / quality control of ACSM measurements

204 Ammonium nitrate calibrations performed on each ACSM are shown in

205 Figure S2. RF_{NO3} and RIE_{NH4} do not present significant seasonal variability - e.g. for ACSM#2 RF_{NO3}=4.7E-

206 11±0.2E-11 A.µg^{-1}.m^3 - , suggesting constant calibration factors may be used throughout the campaign.

207 On the other hand, calibration factors exhibit substantial discrepancies between both ACSMs (e.g. RF_{NO3}

208 of 2.5E-11 and 4.7E-11 A.µg^{-1}.m^3 for ACSM#1 and #2, respectively), suggesting that instrument-specific

209 factors are necessary. Applying constant and composition-dependent CEs does not lead to noticeable

210 differences (e.g. for NR-PM$_1$: r^2=0.97, slope=1.00±0.00, y-intercept=0.10±0.03 µg/m^3, n=14842) due to i)

211 low sampling line RH (e.g. typically below 30% for ACSM#2), and ii) few high-nitrate-content events (only

212 5% of data exhibits ammonium nitrate mass fractions >40%, defined as high by Middlebrook et al., 2012).

213 The Middlebrook et al. (2012) algorithm is however preferred since slightly acidic aerosols are observed

214 at the study site (on average sulfate plus nitrate against ammonium in µeq/m^3: r^2=0.96, slope=1.21±0.00,

215 intercept=0.01±0.00 µeq/m^3, n=14842).

216   A comparison performed between the two ACSMs used in this study during a 2-month summer

217 period is shown in Figure S3. Very good correlations are observed for every chemical component

218 (0.91<r^2<0.98, n=1402, hourly average) - chloride excluded - with slopes relatively close to one

219 (0.87<slopes<1.42), indicating a fairly good comparability between both instruments. One of the two

220 ACSMs also participated in the first-ever inter-ACSM comparison exercise performed between 13

221 different European Q-ACSMs during 3 weeks in Paris, France (Crenn et al., 2015). Satisfactory

222 performances - defined by |z-scores|<2 - are reported for our instrument regarding every chemical

223 component and NR-PM$_1$ mass, attesting the consistency of our measurements with other European sites.

224   Measurements performed by the ACSM and independent off-line and on-line analytical

225   techniques are compared in Figure 1 and Table 1. An overall good agreement is found for every major

226   components throughout the year (typically $r^2>0.8$), although discrepancies are observable for specific

227   species and seasons. On the annual scale, a good agreement ($r^2=0.77$, n=317) is found between organics

228   from ACSM and OC from filter measurements in spite of expected filter sampling artefacts (Maimone et

229   al., 2011; Turpin et al., 2000; Watson et al., 2009). Even better agreements are observed on a seasonal

230   basis (r^2~0.9), with steeper slopes in summer compared with winter, which likely reflects the different

231   degrees of oxygenation of organics among seasons (leading to different OM-to-OC ratios). However, these

232   slopes cannot be directly regarded as the OM-to-OC ratios due to i) differences in size fractions between

233   both methods (PM_1 for ACSM and $PM_{2.5}$ for filter measurements) and ii) uncertainties related to RIE_{Org} for

234   ACSM measurements (Budisulistiorini et al., 2014; Ripoll et al., 2015). An estimation of the OM-to-OC ratio

235   for submicron organics applying the methodology described by Canagaratna et al. (2015) is discussed in

236   Sect. 4.2. Good correlations are observed for nitrate during all seasons ($r^2>0.9$) but summer ($r^2=0.5$), which

237   is most likely related to enhanced evaporative losses of ammonium nitrate from filter during the latter

238   season (Chow et al., 2005; Schaap et al., 2004). Slopes range from 0.9 to 1.4 - summer excluded - which is

239   comparable to what is reported elsewhere (Budisulistiorini et al., 2014; Crenn et al., 2015; Ripoll et al.,

240   2015). Very good correlations are observed for sulfate in every season ($r^2=0.9-1.0$) with slopes close to 1

241   (0.9-1.1, winter excluded), consistent with its presence in the submicronic size fraction and its low

242   volatility leading to the minimization of sampling artefacts. Note that discrepancies have been reported

243   when comparing sulfate measured by the ACSM (Petit et al., 2015) or the AMS (Zhang, 2005) with

244   independent measurements. Our results suggest that ammonium sulfate calibrations should be

245   performed to experimentally determine sulfate RIEs, which appear to be instrument-specific but stable

246   over several months. Although aerosols are slightly acidic on average at the study site, ammonium mostly

247   neutralizes nitrate and sulfate throughout the campaign and thus exhibits behaviour in between the two

248   latter compounds. Higher uncertainties are associated with chloride from filter quantification, resulting in

249   no agreement with ACSM measurements in summer when the concentrations are the lowest ($r^2=0.00$),

250   and fairly good agreement during the other seasons ($r^2=0.64-0.77$). The high slope observed for the

251   ACSM#1 (e.g. 2.1 during spring) compared to the fairly good slopes observed for ACSM#2 (0.7-1.1)

252   suggests that chloride RIE might be instrument-specific and require appropriate calibrations for its

253   accurate quantification (see also Riffault et al., 2013 on this topic).

254   The sum of NR-PM_1 components and BC has been compared to the volume concentration of PM_1.

255   Good agreement is found between both variables ($r^2>0.8$) giving further confidence on the consistency of

256   our ACSM measurements. The annual average particle density estimated from this comparison (i.e. slope)

257   is 1.6, which is typical of ambient aerosol particles densities (1.5-1.9 in Hand and Kreidenweis, 2002; Hu

258   et al., 2012; McMurry et al., 2002; Pitz et al., 2003, 2008). The higher densities observed during spring and

259   summer (1.9-2.0) than autumn and winter (1.3-1.5) are likely due to the enhanced contribution of

260   secondary aerosol and aged particles during the former period (Pitz et al., 2008).

261

262   3.2. Quality assurance / quality control of organic source apportionment

263   First, during the aforementioned inter-ACSM comparison study (Crenn et al., 2015), source

264   apportionment of organics was performed based on data from 13 Q-ACSMs (Fröhlich et al., 2015),

265   including one ACSM used in the present study. Satisfactory performances (|z-scores|<2) are reported for

266   our ACSM using a similar approach as adopted in this study. This result demonstrates that our instrument

267   and the associated data treatment, including the source apportionment modelling, are capable of

268   accurately identifying and quantifying OA sources.

269

270   3.2.1.   Model configurations

271   Regarding our specific study, the configuration applied to reach the optimal SA of organics is

272   thoroughly discussed in Sect. S2 (constrained factor profiles, number of factors, *a*-values and integration-

273   period durations). Briefly, constraining both HOA and BBOA factors result in satisfactory solutions with

274   relevant factor profiles, time series and daily cycles. Other configurations (e.g. unconstrained factors) lead

275   to unsatisfactory results with high seed variability, mixing of factors or absence of key fragments in

276   identified profiles (e.g. absence of *m/z* 43 and 44 in BBOA contrary to what is reported in Heringa et al.,

277   2011, Figure S4). Solutions applying different number of factors are investigated. Three-factors (HOA,

278   BBOA and OOA) are retained during spring, autumn and winter whereas two factors (HOA and OOA) are

279   most suitable during summer. A lower number of factors results in a mixing of them, whereas a higher

280   number generates additional factors - e.g. semi-volatile OOA (SV-OOA) during summer, OOA-BBOA during

281   autumn - which are not satisfactory - e.g. missing fragments or poor correlations with external data, see

282   Table S1. BBOA cannot be clearly identified during summer i.e. in this season agricultural waste burning

283   contributions are estimated to be minor (maximum 3-4% of OA, Sect. S2). Note that COA could not be

284   evidenced, likely due to the type of site studied (regional background) and the lower sensitivity, time- and

285   mass-to-charge-resolution of the ACSM compared to classical AMS instruments (further discussed in Sect.

286   S2; see also Dall'Osto et al., 2015 on this subject). Uncertainties associated with factor contributions are

287   estimated by performing sensitivity tests on *a*-values, which are regarded as the most subjective input

288   parameters. Five scenarios putting very low to very high constraints on the reference factor profiles have
289   been defined (see Table S2). Comparable solutions in terms of relative contributions (Figure S5) and
290   agreement with independent measurements (Table S2) are found when applying low to high constraints
291   following the empiric recommendations of Crippa et al. (2014). Unsatisfactory solutions are generally
292   reached under the extreme scenarios (fully fixed factor profiles and m/z specific standard deviations of
293   reference factor profiles). We decided to apply low constraints (i.e. a-values of 0.1 and 0.5 for HOA and
294   BBOA, respectively) to let as much freedom as possible to our factor profiles while remaining in the range
295   of plausible solutions. SA was performed on 3-months, 6-months and 1-year datasets. Although
296   comparable solutions are found for each configuration (number of factors, factor profiles, diurnal cycles,
297   comparisons with external data), applying SA on seasonal datasets was preferred since i) the seasonal
298   variability of factor profiles is captured and ii) questionable results are observed in summer for 6-months
299   and 1-year configurations (see Sect. S2). When comparing the sum of OA factor concentrations and
300   measured OA on the annual scale, OA is very well modelled (r^2=0.97, slope=0.98±0.00, intercept=0.1±0.0
301   µg/m^3, n=14842).

302

303   3.2.2.   Model optimal solution

304   Factor profiles, contributions and daily cycles of the optimal SA solution are presented in Figure
305   2. Independent factor profiles and time series are found for each season, which is a prerequisite for having
306   reliable SA solutions. HOA is identified during every season and exhibits a profile dominated by alkyl
307   fragments such as m/z 55 (from the $C_nH_{2n-1}^+$ ion series) and m/z 57 (from $C_nH_{2n+1}^+$ ion series; Ng et al.,
308   2011c). Its relative contribution is characteristic of traffic emissions, exhibiting a peak in the morning, and
309   higher contributions during weekdays than weekends (e.g. averages of 14 and 9%, respectively, in
310   autumn, Fig. S6). BBOA is found during every season except summer and has a profile similar to that of
311   HOA, except for the high contribution of m/z 60 ($C_2H_4O_2^+$) and 73 ($C_3H_5O_2^+$), which have been suggested
312   as biomass burning markers (Lee et al., 2010 and references therein). A distinct daily cycle with higher
313   contributions during night-time than daytime is observed, in addition to higher contributions during
314   weekends than weekdays (e.g. averages of 24 and 21%, respectively, in spring, Fig. S6), consistent with
315   residential heating emissions. The low BBOA concentrations modelled during late spring and early
316   autumn, as well as the small increased contribution observed during the morning also suggest residential
317   heating emissions. OOA is identified thanks to the predominant contribution of m/z 44 (CO_2^+) and 43
318   ($C_2H_3O^+$). The higher contribution of f_{44} (defined as m/z 44 to total organic signal; 0.17-0.23 depending on
319   seasons) with respect to f_{43} (defined similarly; 0.05-0.09) suggests that this OOA factor is highly oxidized

320   and presents low volatility (LV-) rather than semi-volatility (SV-) OOA characteristics (see Jimenez et al.,

321   2009 and Zhang et al., 2011 for definitions of these components). This statement is supported by very

322   good correlations (r^2=0.96-0.99) found between our unconstrained OOA profiles and the average low-

323   volatility OOA (LV-OOA) profile reported by Ng et al. (2011c) from 6 AMS studies. Interestingly, our OOA

324   profiles present slight seasonal differences that likely reflect changes in source contributions and/or

325   physical-chemical processes in this factor. For instance, f_{60} in OOA profiles is enhanced in winter (0.014)

326   compared with other seasons (0.001-0.004), which suggests that biomass burning contributes to this

327   factor during the aforementioned season, consistent with different studies reporting f_{60} in secondary OA

328   from biomass burning (e.g. Cubison et al., 2011; Heringa et al., 2011; see Sect. S2). Note that the mass

329   spectral resemblance of primary humic-like substances to LV-OOA might also partly explain this

330   observation (e.g. Young et al., 2015), i.e. that a small fraction of primary OA is found in this factor. Daily

331   cycles are comparable for all seasons with a bimodal pattern characterized by a small peak during night-

332   time and a prominent peak during daytime. The latter peak suggests that a fraction of (LV-) OOA could be

333   locally rather than regionally produced on the time scale of few hours only, likely due to enhanced

334   photochemical activities during daytime. The former peak could be due to i) the condensation of highly

335   oxygenated semi-volatile material favoured by night-time thermodynamic conditions or ii) a contribution

336   of SV-OOA in our OOA factor, which is generally dominated by LV-OOA. The absence of an f_{44} night-time

337   peak (Sect. 4.2) suggests that the second assumption is more probable implying that both SV-OOA and

338   LV-OOA influence our OOA factor.

339

340   3.2.3.   Time series comparisons

341   Comparisons between our OA factors, *m/z* tracer and independent species time series are shown

342   in Table 2. OOA time series show very good agreement with Org_43 (organic signal at *m/z* 43) and Org_44

343   (r^2>0.8 and 0.9, respectively) and relatively good agreement with secondary inorganic species (e.g. $r^2 \geq 0.5$

344   for ammonium), indicating that this factor can be regarded as a surrogate for secondary organic aerosols.

345   Comparisons with sulfate (a low-volatility species) and nitrate (a semi-volatile species) confirm that our

346   OOA factor might be a mix of SV- and LV-OOA, since better agreement is found with one or the other

347   compound depending on the season studied. BBOA exhibits very good coefficients of determination when

348   compared with its presumable fragment tracers Org_60 and Org_73 (r^2>0.97), giving further confidence

349   on its appropriate quantification. Good correlations are generally found between BBOA and BC ($r^2 \geq 0.5$,

350   except for summer) indicating that a large proportion of BC stems from biomass burning, consistent with

351   previous findings at the study site (Gilardoni et al., 2011, from EC measurements). A good agreement is

352 also observed with CO ($r^2 \geq 0.7$), as already reported in the Alpine valleys (e.g. Gaeggeler et al., 2008). HOA

353 is not as well correlated with external data or specific *m/z*, which could be related to i) the absence of

354 clear *m/z* tracers for this factor due to similarities with BBOA profile, ii) the absence of clear external

355 tracers due to co-emissions by fossil fuel and biomass burning activities of BC, CO and NOx and iii) possible

356 uncertainties associated with the apportionment between HOA and BBOA. The first two assumptions are

357 supported by the better agreement observed between HOA and *m/z* fragments or independent data

358 during summer (e.g. r^2=0.52, n=2208 between HOA and BC) and specific months (e.g. May, September),

359 when biomass burning contributions are negligible. Although uncertainties associated with the accurate

360 apportionment of HOA and BBOA cannot be excluded (e.g. due to rotational ambiguity), several factors

361 evidence the robustness of the results and indicate that a mixing of both factors is unlikely, since HOA and

362 BBOA present i) independent factor time series during all seasons (r^2=0.1-0.2), ii) distinct and relevant

363 daily cycles and iii) no significant *a*-value variability.

364

365   4. Results and discussion

366 The meteorological representativeness of this one-year measurement is assessed by comparing the solar

367 irradiation, precipitation, and temperature monthly averages to the ones measured during 1990-2010 at

368 the study site (Figure S7). Comparable seasonal averages are generally found in our study and during the

369 bidecadal reference period. Nevertheless compared to 1990-2010, Spring 2013 was rainier, Summer 2013

370 slightly warmer and sunnier, and Winter 2013-2014 rainier. Further information regarding the

371 representativeness of measurements performed at the study site during the year 2013 can be found in

372 Putaud et al. (2014a).

373

374   4.1. Chemical composition of NR-PM$_1$

375 An overview of the chemical composition of NR-PM$_1$ retrieved during this campaign is shown in Figure 3.

376 The annual averaged NR-PM$_1$ mass reported here (14.2 µg/m^3) ranges amongst the highest NR-PM$_1$ levels

377 (7th out of 41 sites) reported at rural and urban downwind sites in Europe (Crippa et al., 2014) and

378 worldwide (Jimenez et al., 2009; Zhang et al., 2007, 2011). Please note that these previous studies are

379 based on typically one month of measurements in different seasons. It is comparable to NR-PM$_1$ levels

380 reported during specific campaigns in the urban areas of New York City (USA, 12 µg/m^3, Weimer et al.,

381 2006), Tokyo (Japan, 12-15 µg/m^3, Takegawa et al., 2006) or Manchester (UK, 14 µg/m^3, Allan et al., 2003a,

382 2003b). Our annual average NR-PM$_1$ mass is higher than the 10 µg/m^3 guideline given by the World Health

383 Organization for the annual average PM$_{2.5}$ mass (including refractory and non-refractory compounds;

384   WHO, 2006). After similar conclusions have been drawn for $PM_{2.5}$ and PM_{10} size fractions (Putaud et al.,

385   2010), the Po Valley appears to be one of the most polluted regions in Europe with regard to NR-PM_1

386   levels this time. Submicron aerosol particles are mostly made of organics (58%), nitrate (21%), sulfate

387   (12%) and ammonium (8%; Figure 3). The predominance of organics is typical of urban downwind sites

388   (e.g. average of 52% reported in Zhang et al., 2011). On the other hand, the noticeable proportion of

389   nitrate is characteristic of urban sites (18% in Zhang et al., 2011), which likely reflects the substantial

390   influence of anthropogenic activities emissions at our regional site. As a result, sulfate exhibits particularly

391   low contributions at the study site compared with other locations (generally >20% in Zhang et al., 2011).

392   NR-PM_1 levels present a clear seasonality with higher levels during spring (~18 $\mu g/m^3$) and winter

393   (~15 $\mu g/m^3$) compared with summer and autumn (~12 $\mu g/m^3$). Higher levels were expected during cold

394   months due to enhanced biomass burning emissions and lower boundary layer heights (BLH), as

395   previously observed at the study site (Putaud et al., 2013). Expected seasonal variations of the chemical

396   composition of NR-PM_1 are observed, with i) higher nitrate contributions during the cold season which

397   favours its partitioning in the condensed phase (Clegg et al., 1998), ii) higher sulfate contributions during

398   summer, which can e.g. be associated with enhanced photochemical production (Seinfeld and Pandis,

399   2006) and lower amount of rainout (Fig. S7), and iii) relatively stable contributions for ammonium (mainly

400   neutralizing the two previous species) and organics (discussed later on).

401   A focus will now be made on daily cycles of the chemical composition of NR-PM_1 (Figure 4),

402   displayed for the first time during the 4 seasons in the Po Valley, thanks to the high time resolution and

403   stability of the ACSM. On the annual scale, daily cycles of NR-PM_1 levels are characterized by significantly

404   higher concentrations during night-time than daytime, likely due to lower BLH, higher wood burning

405   emissions (during cold seasons) and lower temperatures favouring the partitioning of semi-volatile

406   inorganic (mainly ammonium nitrate) and organic material in the condensed phase, to name a few. A

407   distinct peak is however observed around noon, probably caused by enhanced photochemical production

408   of secondary organic compounds, and increased BLH favouring downward mixing of advected pollution,

409   especially during summer (Figure 4; Decesari et al., 2014). Note that this annual daily pattern is the

410   combination of distinct daily cycles varying with the season studied (Figure 4). In terms of relative chemical

411   composition, organics are dominating NR-PM_1 mass independently of the time of the day, with median

412   contributions ranging from ~60 to 70%. Nitrate exhibits higher contribution during night-time due to its

413   abovementioned semi-volatile nature. Sulfate shows unexpected daily cycles with significantly different

414   (99.99% confidence level) relative contributions - and absolute concentrations - during daytime (~15% of

415   NR-PM_1 mass around noon) compared to night-time (~10% around midnight, Figure 4), although its

416 formation was expected to occur mainly over longer time scales (i.e. days) in cloud droplets (Ervens et al.,

417 2011). This observation could be due to i) local production of sulfate with increased photochemical

418 production around noon at the study site and/or ii) diurnal changes of the atmospheric stratification in

419 the Po Valley as described by Saarikoski et al. (2012) and Decesari et al. (2014), enhancing aged particle

420 contribution during the middle of the day and the afternoon. Non-refractory chloride (mostly NH_4Cl,

421 Huang et al., 2010) exhibits very low contributions independently of the hour of the day (medians below

422 0.5% of $NR\text{-}PM_1$ mass) with however a slight increase at night, which is likely due to its presumable semi-

423 volatile nature here.

424

425   4.2. Focus on organic aerosols

426 An overview of the contribution of HOA, BBOA and OOA to OA is shown in Figure 5. On the annual average,

427 the organic fraction is dominated by the secondary component (OOA, 66%). Although this OOA

428 contribution is substantial, higher proportions are generally reported at rural and urban downwind sites

429 worldwide (90 and 82% of OA on average, respectively, Zhang et al., 2011). This lower relative contribution

430 of OOA is related to the higher contribution of (primary) BBOA in our study (23% of OA on the annual

431 average) compared to the previous ones. Considerable contributions of BBOA are explained by the specific

432 location of the study site in the vicinity of the Alps, where biomass burning is a major contributor to OA

433 (Belis et al., 2011; Herich et al., 2014; Lanz et al., 2010). Biomass burning emissions hence substantially

434 affect OA levels on the annual scale here. The contribution of HOA is comparatively smaller (11%),

435 indicating that despite the expected large contributions of fossil fuel emissions (i.e. traffic and industrial

436 emissions), those are not the major sources of primary OA at the study site. On the other hand, it is likely

437 that fossil fuel emissions of volatile organic compounds (VOCs) - which are OOA precursors - contribute

438 to our OOA levels as reported elsewhere (Gentner et al., 2012; Volkamer et al., 2006). At the study site,

439 Gilardoni et al. (2011) previously estimated on the basis of ^{14}C analyses that secondary organic carbon

440 stemming from fossil emissions might represent 12% of OC on the annual average. In other words, fossil

441 fuel emissions could represent approximately a quarter (12+11=23%) of total OA mass when both primary

442 and secondary OA fractions are accounted for. The analysis of the components' seasonal variations shows

443 relatively stable HOA contributions (9-14%), higher contributions of BBOA during cold seasons due to

444 residential heating (up to 36% of OA on average during winter) and higher OOA contributions during

445 summer related to enhanced photochemical production (86% of OA on average).

446   OA can be further characterized investigating specific organic fragments. m/z 44 (mainly CO_2^+)

447 and 43 (mainly $C_2H_3O^+$) signals give insights on the nature of OA, as the former is primarily related to acids

448   or acid-derived species whereas the latter is mostly associated with non-acid oxygenates (Duplissy et al.,

449   2011; Ng et al., 2011b). Daily variations of both f_{44} and f_{43} are shown in Figure 6, along with other major

450   organic fragments. On average, f_{44} is predominant with respect to f_{43} (15 and 7%, respectively), which

451   indicates that acid species dominate the OA composition with respect to non-acid oxygenates. Both

452   fragments present different daily patterns underlying distinct mechanisms of formation. Acids'

453   contributions are enhanced during daytime, which could be explained by photochemical processes and/or

454   daily BLH variations as already discussed for sulfate. Non-acid oxygenates exhibit higher contributions

455   during night-time than daytime. This pattern could be due to i) the formation of semi-volatile non-acids

456   during night-time by e.g. condensation (Lanz et al., 2007), ii) their degradation during daytime by e.g.

457   fragmentation reactions (Daumit et al., 2013) and/or iii) their conversion into acid-related species during

458   daytime by e.g. functionalization or oligomerization reactions (Daumit et al., 2013). It should be specified

459   that the enhancement of f_{44} during daytime and the increasing of f_{43} during night-time only represent a

460   small fraction of their total contributions to OA (Figure 6), suggesting that most acid and non-acid

461   oxygenates have been formed before reaching our sampling site, i.e. have been imported from other

462   regions. The other major OA fragments (m/z 29, 55, 57 and 60) present i) constant contributions for f_{29}

463   due its various emission sources (HOA, BBOA, OOA; Ng et al., 2011c), ii) the absence of lunch peak for f_{55}

464   (and also for the absolute contributions of m/z 55) consistent with the presumable low influence of

465   cooking emissions, iii) morning and evening peaks for f_{57} characteristic of fossil fuel emissions and iv)

466   higher contributions during night-time for f_{60} in agreement with its biomass burning origin.

467   Using f_{43} and f_{44}, the oxygen-to-carbon (O/C), OM-to-OC (OM/OC), hydrogen-to-carbon (H/C)

468   ratios and the carbon oxidation state (OSc) have been estimated for total OA based on the methodologies

469   described by Aiken et al. (2008), Kroll et al. (2011) and Ng et al. (2011b), and applying the parameterization

470   defined in Canagaratna et al. (2015), which can be summarized as follows:

471   O/C= 4.31 f_{44}+ 0.079   (1)

472   OM/OC= 1.28 O/C+ 1.17   (2)

473   H/C= 1.12+ 6.74 f_{43} - 17.77 f_{43}^2 (3)

474   OSc=2*O/C-H/C   (4)

475   with H/C (and therefore OSc) being estimated only if f_{44}>0.05 and f_{43}>0.04 (Canagaratna et al., 2015).

476   Uncertainties associated with these estimates - in particular based on ACSM measurements - are

477   discussed in Sect. S3 (see also Fig. S8). Comparisons with studies using (HR-ToF-) AMS instruments will not

478   be reported and only variations within this dataset will be discussed (see Sect. S3). Seasonal and annual

479   O/C, OM/OC, H/C and OSc are shown in Figure 7. High O/C, OM/OC and OSc are found on the annual scale

480   (medians of 0.7, 2.1 and -0.2, respectively), reflecting once more the aged, oxidized properties of organic

481   matter at the study site, consistent with the predominance of the OOA component. Little seasonal

482   variations are observed for the aforementioned variables hence highlighting the high degree of oxidation

483   of OA throughout the year (Figure 7). The unexpectedly high degree of oxygenation of OA observed during

484   cold seasons despite the increased contribution of primary BBOA (with OM/OC ratios of 1.4-1.6) could be

485   explained by the contribution of secondary BBOA in our OOA factor during these cold seasons, which

486   could be associated with the enhancement of e.g. dicarboxylic and ketocarboxylic acid contents (Kundu

487   et al., 2010) that have extremely high OM/OC ratios (up to 3.8 and 3.1, respectively, Turpin and Lim, 2001).

488   This assumption is supported by the higher proportion of f_{60} in our OOA factor (discussed in Sect. 3.2 and

489   S2), as well as the surprisingly high OM/OC ratio observed for OOA during winter (2.5 compared to 2.2-

490   2.4 during the other seasons). Note that Canonaco et al. (2015) also report a higher f_{44} in (LV-) OOA in

491   winter compared to summer in Zurich (Switzerland). According to these authors, this could be due to

492   enhanced aqueous-phase production of (LV-) OOA in clouds or hygroscopic aerosols in winter, which

493   would lead to higher levels of oxygenation compared to gas-phase oxidation mechanisms typically

494   occurring during summer.

495

496   4.3. Possible implications for PM abatement strategies

497   In order to investigate the characteristics of fine aerosol pollution events, the variations of NR-PM$_1$

498   chemical composition and OA factors' contributions as a function of total NR-PM$_1$ mass are examined.

499   This investigation is made on the annual (Figure 8, discussion below) and seasonal scales (Fig. S9,

500   discussion in Sect. S4). Distinct trends are observed depending on the chemical species and OA

501   components studied. The proportion of nitrate is clearly enhanced with increasing NR-PM$_1$ levels (from

502   ~10 to >30% when [NR-PM$_1$]>30 µg/m^3) indicating that nitrate - or NO$_x$ - abatement policies should be

503   highly effective when attempting to limit PM$_1$ pollution events in the Upper Po Valley. Sulfate shows an

504   opposite trend with decreasing relative contribution when NR-PM$_1$ mass increases (e.g. <5% when [NR-

505   PM$_1$]> 50 µg/m^3), likely due to the lower concentrations of sulfate during cold seasons, when the highest

506   number of pollution events is observed. The proportion of organics is substantial (48-66%) independently

507   of NR-PM$_1$ mass, justifying once again the importance of determining its sources to design adequate

508   abatement policies. When focusing on the organic fraction, BBOA is the only OA factor exhibiting

509   increased contributions (from ~10 to >40%) with increased NR-PM$_1$ mass (from <10 to >60 µg/m^3), which

510   points out the PM abatement potential of effective biomass burning emission reductions. HOA levels are

511   rather constant throughout the year and therefore their proportions steadily decrease when NR-PM$_1$

512   levels increase, implying that local fossil fuel related emissions of primary OC are not the main responsible

513   for submicron pollution events observed at the study site on the annual scale. Although OOA always

514   represents a major fraction of OA (41-75% depending on the mass bin studied), its contribution steadily

515   decreases with increasing NR-PM$_1$ mass. This unexpected result signifies that even though aged,

516   secondary, oxidised organics are the main contributor to OA on the annual average (66%), they do not

517   play a prominent role in fine PM acute pollution events.

518   Current European legislations set daily and/or annual PM limit values depending on the size fraction

519   addressed (Directive 2008/50/EC). Volume size distributions suggest that approximately 90% of the PM$_{2.5}$

520   mass concentration is borne by particles below an aerodynamic diameter of 1 µm at the study site (Putaud

521   et al., 2014a). Therefore, measures tackling the main constituents of the submicron aerosol fraction would

522   be efficient for complying with PM$_{2.5}$ legislations. Based on the chemical characterization of NR-PM$_1$ and

523   SA of its organic fraction with a time-resolution of 30 min over 1-year, this study provides new evidence

524   which could orient PM abatement strategies also at similar regional background sites of the Po Valley. On

525   the annual scale, OA and especially OOA should be of main concern given their predominance in NR-PM$_1$

526   chemical composition (Figure 3). On the seasonal scale, efforts should be directed towards the cold

527   seasons (winter and early spring), for which the highest NR-PM$_1$ levels are observed, due to specific

528   meteorological conditions (e.g. low BLH, low temperatures) and emission sources (e.g. biomass burning,

529   Figure 3 and Figure 5). In particular, measures addressing emissions of NO$_x$ and BBOA would be the most

530   efficient for reducing the magnitude and frequency of PM pollution events (Figure 8).

531   Recommendations for PM abatement strategies are formulated here from a legislative perspective,

532   which aims at decreasing PM levels. Although diminishing PM levels should help reducing PM impacts,

533   the existence of a direct causal relationship can be debatable since each chemical component has a

534   specific effect on human health (WHO, 2013), the radiative forcing (Boucher et al., 2013) or ecosystems

535   (e.g. Carslaw et al., 2010). For instance, implementing policies aiming at mitigating nitrate concentrations

536   - as suggested previously in this section - would likely have limited health benefits according to

537   toxicological studies (Reiss et al., 2007; Schlesinger and Cassee, 2003), and should lead to an increased

538   global warming (Boucher et al., 2013). On the other hand, measures reducing BBOA levels should be

539   beneficial, since the cardio-vascular effects of biomass burning particles have been widely reported in the

540   literature (Bølling et al., 2009; Miljevic et al., 2010; Naeher et al., 2007) and could be similar to those of

541   traffic-emitted particles (WHO, 2013 and references therein), whereas their impacts on the radiative

542   forcing could be null (Boucher et al., 2013). Strategies aiming at reducing solely PM mass are therefore

543   limited, and an assessment of their impacts - e.g. using integrated assessment models (Carnevale et al.,

544 2012; Janssen et al., 2009) with appropriate parameterizations of fundamental processes - would be

545 beneficial.

546

547   5.   Conclusion and perspectives

548 The NR-PM$_1$ chemical composition and the apportionment of the organic fraction have been investigated

549 for the first time with this completeness at a regional background site of the Po valley (Italy), using high

550 time-resolution (30 min) and long term (1 year) measurements with a state-of-the-art quality assured

551 ACSM and the most advanced factor analysis methods. Comparisons between two ACSMs show very good

552 time series correlations for the major compounds (0.91<r^2<0.98, n=1402) with however discrepancies in

553 their absolute concentrations (0.9<slopes<1.4). These results are promising with regard to the consistency

554 of ACSM measurements at different locations, but also underlines the importance of conducting inter-

555 ACSM comparisons to define common protocols and assure data comparability among the European

556 ACSM network (see Crenn et al., 2015). Comparisons between ACSM and independent analytical

557 technique measurements show an overall good agreement for major components throughout the year

558 (typically r^2>0.8). Discrepancies observed in time series correlations and quantifications (i.e. slopes) for

559 specific species and seasons (e.g. nitrate in summer) are attributed to filter sampling artefacts. These

560 results are encouraging regarding the potential implementation of ACSMs in air quality networks as a

561 replacement of traditional filter-based techniques, to measure the artefact-free chemical composition of

562 fine aerosols with high time-resolution. Additional comparison studies are nevertheless needed to

563 support our results, and further technical development allowing the refractory carbon fraction to be

564 accounted for is required.

565   NR-PM$_1$ and PM$_1$ levels measured in the upper Po Valley (14.2 and 15.3 µg/m^3 on the annual

566 average, respectively) are among the highest reported in Europe, stressing the need for implementing

567 effective PM abatement strategies in this region. On average, the chemical composition of non-refractory

568 submicron aerosol is dominated by organic aerosol (58% of NR-PM$_1$), which is composed of HOA (11% of

569 OA), BBOA (23%) and OOA (66%). Fossil fuel combustion is thus not a major source of primary OA in this

570 area of the Po Valley. Primary BBOA significantly contributes to OA on the annual average and especially

571 during winter (36%). Our OOA component is highly oxidised and aged with an LV-OOA spectral signature,

572 a large proportion of acid-related species and high OM/OC ratios. Highly oxidised OA properties are

573 observed during all seasons, surprisingly including winter, which could reflect secondary BBOA influence

574 and OOA aqueous-phase formation processes during cold seasons. Further research aiming at identifying

575 the sources of OOA - including secondary BBOA using e.g. high resolution mass spectrometric techniques

576 (Crippa et al., 2013) or proton nuclear magnetic resonance (Paglione et al., 2014) - and better estimating

577 O/C, OM/OC and OSc parameters would be beneficial.

578 Specific recommendations for PM abatement strategies at a regional level can be suggested. The

579 higher frequency of particulate pollution peaks observed during cold seasons suggests an orientation of

580 future policies towards these periods. BBOA and nitrate present increasing relative contributions with

581 increasing fine aerosol levels, which suggests that wood burning and NO_x emission reductions should

582 notably decrease NR-PM_1 pollution events. Note that these recommendations are only formulated in the

583 perspective of reducing PM levels, assuming a subsequent reduction of PM impacts. Additional

584 dimensions - e.g. specific impacts of each chemical component, short versus long-term exposure, co-

585 benefit of sanitary and climatic impacts - should also be considered when defining PM abatement

586 strategies. In a broader context, the use of high time resolution analytical techniques for the measurement

587 of PM pollution properties can help better shape our future air quality policies.

588

589 *Acknowledgements.* This study was partially supported by the European Union's project ACTRIS (Aerosols,

590 Clouds, and Trace gases Research InfraStructure Network, EU FP7-262254). R. Passarella (EC-JRC), K.

591 Douglas (EC-JRC), V. Pedroni (EC-JRC) and M. Stracquadanio (ENEA) are thanked for their help on the field

592 and/or for the chemical analyses of filters. P. Croteau (Aerodyne) is acknowledged for his technical

593 support on the operation of the ACSM. N. Jensen (EC-JRC) is thanked for providing gas phase data. M.

594 Crippa (EC-JRC) is acknowledged for her valuable advices.

References

Aerodyne: Aerosol Chemical Speciation Monitor: Data Acquisition Software Manual, available at: ftp://ftp.aerodyne.com/ACSM/ACSM_Manuals/ACSM_DAQ_Manual.pdf (last access: 15 February 2016), 2010a.

Aerodyne: Aerosol Chemical Speciation Monitor: Data Analysis Software Manual, available at: ftp://ftp.aerodyne.com/ACSM/ACSM_Manuals/ACSM_Igor_Manual.pdf (last access: 15 February 2016), 2010b.

Aiken, A. C., DeCarlo, P. F., Kroll, J. H., Worsnop, D. R., Huffman, J. A., Docherty, K. S., Ulbrich, I. M., Mohr, C., Kimmel, J. R., Sueper, D., Sun, Y., Zhang, Q., Trimborn, A., Northway, M., Ziemann, P. J., Canagaratna, M. R., Onasch, T. B., Alfarra, M. R., Prevot, A. S. H., Dommen, J., Duplissy, J., Metzger, A., Baltensperger, U., and Jimenez, J. L.: O/C and OM/OC ratios of primary, secondary, and ambient organic aerosols with high-resolution time-of-flight aerosol mass spectrometry, Environ. Sci. Technol., 42(12), 4478–4485, doi:10.1021/es703009q, 2008.

Allan, J. D., Jimenez, J. L., Williams, P. I., Alfarra, M. R., Bower, K. N., Jayne, J. T., Coe, H., and Worsnop, D. R.: Quantitative sampling using an Aerodyne aerosol mass spectrometer 1. Techniques of data interpretation and error analysis, J. Geophys. Res.-Atmos., 108(D3), 4090, doi:10.1029/2002JD002358, 2003a.

Allan, J. D., Alfarra, M. R., Bower, K. N., Williams, P. I., Gallagher, M. W., Jimenez, J. L., McDonald, A. G., Nemitz, E., Canagaratna, M. R., Jayne, J. T., Coe, H., and Worsnop, D. R.: Quantitative sampling using an Aerodyne aerosol mass spectrometer 2. Measurements of fine particulate chemical composition in two U.K. cities, J. Geophys. Res.-Atmos., 108(D3), 4091, doi:10.1029/2002JD002359, 2003b.

Amato, F., Pandolfi, M., Escrig, A., Querol, X., Alastuey, A., Pey, J., Perez, N., and Hopke, P. K.: Quantifying road dust resuspension in urban environment by Multilinear Engine: a comparison with PMF2, Atmos. Environ., 43(17), 2770–2780, doi:10.1016/j.atmosenv.2009.02.039, 2009.

Belis, C. A., Cancelinha, J., Duane, M., Forcina, V., Pedroni, V., Passarella, R., Tanet, G., Douglas, K., Piazzalunga, A., Bolzacchini, E., Sangiorgi, G., Perrone, M.-G., Ferrero, L., Fermo, P., and Larsen, B. R.: Sources for PM air pollution in the Po Plain, Italy: I. Critical comparison of methods for estimating biomass burning contributions to benzo(a)pyrene, Atmos. Environ., 45(39), 7266–7275, doi:10.1016/j.atmosenv.2011.08.061, 2011.

Belis, C. A., Karagulian, F., Larsen, B. R., and Hopke, P. K.: Critical review and meta-analysis of ambient particulate matter source apportionment using receptor models in Europe, Atmos. Environ., 69, 94–108, doi:10.1016/j.atmosenv.2012.11.009, 2013.

Bølling, A. K., Pagels, J., Yttri, K., Barregard, L., Sallsten, G., Schwarze, P. E., and Boman, C.: Health effects of residential wood smoke particles: the importance of combustion conditions and physicochemical particle properties, Part. Fibre Toxicol., 6(1), 29, doi:10.1186/1743-8977-6-29, 2009.

Boucher, O., Randall, D., Artaxo, P., Bretherton, C., Feingold, G., Forster, P., Kerminen, V.-M., Kondo, Y., Liao, H., Lohmann, U., Rasch, P., Satheesh, S. K., Sherwood, S., Stevens, B., and Zhang, X.: Clouds and aerosols, in Climate Change 2013: The Physical Science Basis. Contribution of Working Group I to the Fifth Assessment Report of the Intergovernmental Panel on Climate Change, edited by: Stocker, T. F., Qin, D., Plattner, G.-K., Tignor, M., Allen, S. K., Boschung, J., Nauels, A., Xia, Y., Bex, V., and Midgley, P. M., Cambridge University Press, Cambridge, United Kingdom and New York, NY, USA, 2013.

Budisulistiorini, S. H., Canagaratna, M. R., Croteau, P. L., Marth, W. J., Baumann, K., Edgerton, E. S., Shaw, S. L., Knipping, E. M., Worsnop, D. R., Jayne, J. T., Gold, A., and Surratt, J. D.: Real-time continuous

characterization of secondary organic aerosol derived from isoprene epoxydiols in downtown Atlanta, Georgia, using the Aerodyne aerosol chemical speciation monitor, Environ. Sci. Technol., 47(11), 5686–5694, doi:10.1021/es400023n, 2013.

Budisulistiorini, S. H., Canagaratna, M. R., Croteau, P. L., Baumann, K., Edgerton, E. S., Kollman, M. S., Ng, N. L., Verma, V., Shaw, S. L., Knipping, E. M., Worsnop, D. R., Jayne, J. T., Weber, R. J., and Surratt, J. D.: Intercomparison of an aerosol chemical speciation monitor (ACSM) with ambient fine aerosol measurements in downtown Atlanta, Georgia, Atmos. Meas. Tech., 7(7), 1929–1941, doi:10.5194/amt-7-1929-2014, 2014.

Canagaratna, M. R., Jayne, J. T., Jimenez, J. L., Allan, J. D., Alfarra, M. R., Zhang, Q., Onasch, T. B., Drewnick, F., Coe, H., Middlebrook, A., Delia, A., Williams, L. R., Trimborn, A. M., Northway, M. J., DeCarlo, P. F., Kolb, C. E., Davidovits, P., and Worsnop, D. R.: Chemical and microphysical characterization of ambient aerosols with the Aerodyne aerosol mass spectrometer, Mass Spectrom. Rev., 26(2), 185–222, doi:10.1002/mas.20115, 2007.

Canagaratna, M. R., Jimenez, J. L., Kroll, J. H., Chen, Q., Kessler, S. H., Massoli, P., Hildebrandt Ruiz, L., Fortner, E., Williams, L. R., Wilson, K. R., Surratt, J. D., Donahue, N. M., Jayne, J. T., and Worsnop, D. R.: Elemental ratio measurements of organic compounds using aerosol mass spectrometry: characterization, improved calibration, and implications, Atmos. Chem. Phys., 15, 253–272, doi:10.5194/acp-15-253-2015, 2015.

Canonaco, F., Crippa, M., Slowik, J. G., Baltensperger, U., and Prévôt, A. S. H.: SoFi, an IGOR-based interface for the efficient use of the generalized multilinear engine (ME-2) for the source apportionment: ME-2 application to aerosol mass spectrometer data, Atmos. Meas. Tech., 6(12), 3649–3661, doi:10.5194/amt-6-3649-2013, 2013.

Canonaco, F., Slowik, J. G., Baltensperger, U., and Prévôt, A. S. H.: Seasonal differences in oxygenated organic aerosol composition: implications for emissions sources and factor analysis, Atmos. Chem. Phys., 15(12), 6993–7002, doi:10.5194/acp-15-6993-2015, 2015.

Carbone, C., Decesari, S., Paglione, M., Giulianelli, L., Rinaldi, M., Marinoni, A., Cristofanelli, P., Didiodato, A., Bonasoni, P., Fuzzi, S., and Facchini, M. C.: 3-year chemical composition of free tropospheric PM_1 at the Mt. Cimone GAW global station – South Europe – 2165 m a.s.l., Atmos. Environ., 87, 218–227, doi:10.1016/j.atmosenv.2014.01.048, 2014.

Carnevale, C., Finzi, G., Pisoni, E., Volta, M., Guariso, G., Gianfreda, R., Maffeis, G., Thunis, P., White, L., and Triacchini, G.: An integrated assessment tool to define effective air quality policies at regional scale, Environ. Modell. Softw., 38, 306–315, doi:10.1016/j.envsoft.2012.07.004, 2012.

Carslaw, K. S., Boucher, O., Spracklen, D. V., Mann, G. W., Rae, J. G. L., Woodward, S., and Kulmala, M.: A review of natural aerosol interactions and feedbacks within the Earth system, Atmos. Chem. Phys., 10(4), 1701–1737, 2010.

Cavalli, F., Viana, M., Yttri, K. E., Genberg, J., and Putaud, J. P.: Toward a standardised thermal-optical protocol for measuring atmospheric organic and elemental carbon: the EUSAAR protocol, Atmos. Meas. Tech., 3, 79–89, 2010.

Chow, J. C., Watson, J. G., Lowenthal, D. H., and Magliano, K. L.: Loss of $PM_{2.5}$ nitrate from filter samples in central California, J. Air Waste Manage. Assoc., 55(8), 1158–1168, doi:10.1080/10473289.2005.10464704, 2005.

Clegg, S. L., Brimblecombe, P., and Wexler, A. S.: Thermodynamic model of the system $H^+–NH_4^+–SO_4^{2-}–NO_3^-–H_2O$ at tropospheric temperatures, J. Phys. Chem. A, 102(12), 2137–2154, doi:10.1021/jp973042r, 1998.

Clerici, M. and Mélin, F.: Aerosol direct radiative effect in the Po Valley region derived from AERONET measurements, Atmos. Chem. Phys., 8(16), 4925–4946, 2008.

Crawford, J., Cohen, D., Dyer, L., and Zahorowski, W.: Receptor modelling with PMF2 and ME2 using aerosol data from Hong Kong, Australian Nuclear Science and Technology Organisation (ANSTO),

690   available at: http://apo.ansto.gov.au/dspace/bitstream/10238/201/1/ANSTO-E-756.pdf (last
691   access: 15 February 2016), 2005.
692   Crenn, V., Sciare, J., Croteau, P. L., Verlhac, S., Fröhlich, R., Belis, C. A., Aas, W., Äijälä, M., Alastuey, A.,
693   Artiñano, B., Baisnée, D., Bonnaire, N., Bressi, M., Canagaratna, M., Canonaco, F., Carbone, C.,
694   Cavalli, F., Coz, E., Cubison, M. J., Esser-Gietl, J. K., Green, D. C., Gros, V., Heikkinen, L., Herrmann,
695   H., Lunder, C., Minguillón, M. C., Močnik, G., O'Dowd, C. D., Ovadnevaite, J., Petit, J.-E., Petralia,
696   E., Poulain, L., Priestman, M., Riffault, V., Ripoll, A., Sarda-Estève, R., Slowik, J. G., Setyan, A.,
697   Wiedensohler, A., Baltensperger, U., Prévôt, A. S. H., Jayne, J. T., and Favez, O.: ACTRIS ACSM
698   intercomparison – part 1: reproducibility of concentration and fragment results from 13 individual
699   quadrupole aerosol chemical speciation monitors (Q-ACSM) and consistency with co-located
700   instruments, Atmos. Meas. Tech., 8(12), 5063–5087, doi:10.5194/amt-8-5063-2015, 2015.
701   Crippa, M., DeCarlo, P. F., Slowik, J. G., Mohr, C., Heringa, M. F., Chirico, R., Poulain, L., Freutel, F., Sciare,
702   J., Cozic, J., Di Marco, C. F., Elsasser, M., Nicolas, J. B., Marchand, N., Abidi, E., Wiedensohler, A.,
703   Drewnick, F., Schneider, J., Borrmann, S., Nemitz, E., Zimmermann, R., Jaffrezo, J.-L., Prévôt, A. S.
704   H., and Baltensperger, U.: Wintertime aerosol chemical composition and source apportionment
705   of the organic fraction in the metropolitan area of Paris, Atmos. Chem. Phys., 13(2), 961–981,
706   doi:10.5194/acp-13-961-2013, 2013.
707   Crippa, M., Canonaco, F., Lanz, V. A., Äijälä, M., Allan, J. D., Carbone, S., Capes, G., Ceburnis, D., Dall'Osto,
708   M., Day, D. A., DeCarlo, P. F., Ehn, M., Eriksson, A., Freney, E., Hildebrandt Ruiz, L., Hillamo, R.,
709   Jimenez, J. L., Junninen, H., Kiendler-Scharr, A., Kortelainen, A.-M., Kulmala, M., Laaksonen, A.,
710   Mensah, A. A., Mohr, C., Nemitz, E., O'Dowd, C., Ovadnevaite, J., Pandis, S. N., Petäjä, T., Poulain,
711   L., Saarikoski, S., Sellegri, K., Swietlicki, E., Tiitta, P., Worsnop, D. R., Baltensperger, U., and Prévôt,
712   A. S. H.: Organic aerosol components derived from 25 AMS data sets across Europe using a
713   consistent ME-2 based source apportionment approach, Atmos. Chem. Phys., 14(12), 6159–6176,
714   doi:10.5194/acp-14-6159-2014, 2014.
715   Cubison, M. J., Ortega, A. M., Hayes, P. L., Farmer, D. K., Day, D., Lechner, M. J., Brune, W. H., Apel, E.,
716   Diskin, G. S., Fisher, J. A., Fuelberg, H. E., Hecobian, A., Knapp, D. J., Mikoviny, T., Riemer, D.,
717   Sachse, G. W., Sessions, W., Weber, R. J., Weinheimer, A. J., Wisthaler, A., and Jimenez, J. L.:
718   Effects of aging on organic aerosol from open biomass burning smoke in aircraft and laboratory
719   studies, Atmos. Chem. Phys., 11(23), 12049–12064, doi:10.5194/acp-11-12049-2011, 2011.
720   Dall'Osto, M., Paglione, M., Decesari, S., Facchini, M. C., O'Dowd, C., Plass-Duellmer, C., and Harrison, R.
721   M.: On the Origin of AMS "Cooking Organic Aerosol" at a Rural Site, Environ. Sci. Technol., 49(24),
722   13964–13972, doi:10.1021/acs.est.5b02922, 2015.
723   Daumit, K. E., Kessler, S. H., and Kroll, J. H.: Average chemical properties and potential formation pathways
724   of highly oxidized organic aerosol, Faraday Discuss., 165, 181, doi:10.1039/c3fd00045a, 2013.
725   Decesari, S., Allan, J., Plass-Duelmer, C., Williams, B. J., Paglione, M., Facchini, M. C., O'Dowd, C.,
726   Harrison, R. M., Gietl, J. K., Coe, H., Giulianelli, L., Gobbi, G. P., Lanconelli, C., Carbone, C.,
727   Worsnop, D., Lambe, A. T., Ahern, A. T., Moretti, F., Tagliavini, E., Elste, T., Gilge, S., Zhang, Y., and
728   Dall'Osto, M.: Measurements of the aerosol chemical composition and mixing state in the Po
729   Valley using multiple spectroscopic techniques, Atmos. Chem. Phys., 14, 12109–12132,
730   doi:10.5194/acp-14-12109-2014, 2014.
731   Duplissy, J., DeCarlo, P. F., Dommen, J., Alfarra, M. R., Metzger, A., Barmpadimos, I., Prevot, A. S. H.,
732   Weingartner, E., Tritscher, T., Gysel, M., Aiken, A. C., Jimenez, J. L., Canagaratna, M. R., Worsnop,
733   D. R., Collins, D. R., Tomlinson, J., and Baltensperger, U.: Relating hygroscopicity and composition
734   of organic aerosol particulate matter, Atmos. Chem. Phys., 11(3), 1155–1165, doi:10.5194/acp-
735   11-1155-2011, 2011.
736   EC: Commission of the European communities, Commission staff working paper, Annex to the
737   communication on thematic strategy on air pollution and the directive on "Ambient air quality

738	and cleaner air for Europe", Impact assessment, SEC (2005) 1133, available at:
739	http://ec.europa.eu/environment/archives/cafe/pdf/ia_report_en050921_final.pdf (last access:
740	15 February 2016), 2005.
741	EEA: Air quality in Europe - 2013 report, European Environment Agency (EEA), report no 9/2013,
742	publication, available at: http://www.eea.europa.eu/publications/air-quality-in-europe-2013
743	(last access: 15 February 2016), 2013.
744	Ervens, B., Turpin, B. J., and Weber, R. J.: Secondary organic aerosol formation in cloud droplets and
745	aqueous particles (aqSOA): a review of laboratory, field and model studies, Atmos. Chem. Phys.,
746	11(21), 11069–11102, doi:10.5194/acp-11-11069-2011, 2011.
747	EU: Directive 2008/50/EC of the European Parliament and of the Council of 21 May 2008 on ambient air
748	quality and cleaner air for Europe, available at http://eur-lex.europa.eu/legal-
749	content/en/ALL/?uri=CELEX:32008L0050 (last access 18 July 2016), 2008.
750	Ferrero, L., Castelli, M., Ferrini, B. S., Moscatelli, M., Perrone, M. G., Sangiorgi, G., D'Angelo, L., Rovelli, G.,
751	Moroni, B., Scardazza, F., Močnik, G., Bolzacchini, E., Petitta, M., and Cappelletti, D.: Impact of
752	black carbon aerosol over Italian basin valleys: high-resolution measurements along vertical
753	profiles, radiative forcing and heating rate, Atmos. Chem. Phys., 14(18), 9641–9664,
754	doi:10.5194/acp-14-9641-2014, 2014.
755	Fröhlich, R., Crenn, V., Setyan, A., Belis, C. A., Canonaco, F., Favez, O., Riffault, V., Slowik, J. G., Aas, W.,
756	Aijälä, M., Alastuey, A., Artiñano, B., Bonnaire, N., Bozzetti, C., Bressi, M., Carbone, C., Coz, E.,
757	Croteau, P. L., Cubison, M. J., Esser-Gietl, J. K., Green, D. C., Gros, V., Heikkinen, L., Herrmann, H.,
758	Jayne, J. T., Lunder, C. R., Minguillón, M. C., Močnik, G., O'Dowd, C. D., Ovadnevaite, J., Petralia,
759	E., Poulain, L., Priestman, M., Ripoll, A., Sarda-Estève, R., Wiedensohler, A., Baltensperger, U.,
760	Sciare, J., and Prévôt, A. S. H.: ACTRIS ACSM intercomparison – part 2: intercomparison of ME-2
761	organic source apportionment results from 15 individual, co-located aerosol mass spectrometers,
762	Atmos. Meas. Tech., 8(6), 2555–2576, doi:10.5194/amt-8-2555-2015, 2015.
763	Gaeggeler, K., Prevot, A. S. H., Dommen, J., Legreid, G., Reimann, S., and Baltensperger, U.: Residential
764	wood burning in an Alpine valley as a source for oxygenated volatile organic compounds,
765	hydrocarbons and organic acids, Atmos. Environ., 42(35), 8278–8287,
766	doi:10.1016/j.atmosenv.2008.07.038, 2008.
767	Gentner, D. R., Isaacman, G., Worton, D. R., Chan, A. W. H., Dallmann, T. R., Davis, L., Liu, S., Day, D. A.,
768	Russell, L. M., Wilson, K. R., Weber, R., Guha, A., Harley, R. A., and Goldstein, A. H.: Elucidating
769	secondary organic aerosol from diesel and gasoline vehicles through detailed characterization of
770	organic carbon emissions, Proc. Natl. Acad. Sci. USA, 109(45), 18318–18323,
771	doi:10.1073/pnas.1212272109, 2012.
772	Gilardoni, S., Vignati, E., Cavalli, F., Putaud, J. P., Larsen, B. R., Karl, M., Stenström, K., Genberg, J., Henne,
773	S., and Dentener, F.: Better constraints on sources of carbonaceous aerosols using a combined ^{14}C
774	– macro tracer analysis in a European rural background site, Atmos. Chem. Phys., 11(12), 5685–
775	5700, doi:10.5194/acp-11-5685-2011, 2011.
776	Gilardoni, S., Massoli, P., Giulianelli, L., Rinaldi, M., Paglione, M., Pollini, F., Lanconelli, C., Poluzzi, V.,
777	Carbone, S., Hillamo, R., Russell, L. M., Facchini, M. C., and Fuzzi, S.: Fog scavenging of organic and
778	inorganic aerosol in the Po Valley, Atmos. Chem. Phys., 14(13), 6967–6981, doi:10.5194/acp-14-
779	6967-2014, 2014.
780	Hand, J. L. and Kreidenweis, S. M.: A new method for retrieving particle refractive index and effective
781	density from aerosol size distribution data, Aerosol Sci. Tech., 36(10), 1012–1026,
782	doi:10.1080/02786820290092276, 2002.
783	Herich, H., Gianini, M. F. D., Piot, C., Močnik, G., Jaffrezo, J.-L., Besombes, J.-L., Prévôt, A. S. H., and Hueglin,
784	C.: Overview of the impact of wood burning emissions on carbonaceous aerosols and PM in large

785   parts of the Alpine region, Atmos. Environ., 89, 64–75, doi:10.1016/j.atmosenv.2014.02.008,
786   2014.

787 Heringa, M. F., DeCarlo, P. F., Chirico, R., Tritscher, T., Dommen, J., Weingartner, E., Richter, R., Wehrle,
788   G., Prévôt, A. S. H., and Baltensperger, U.: Investigations of primary and secondary particulate
789   matter of different wood combustion appliances with a high-resolution time-of-flight aerosol
790   mass spectrometer, Atmos. Chem. Phys., 11(12), 5945–5957, doi:10.5194/acp-11-5945-2011,
791   2011.

792 Hu, M., Peng, J., Sun, K., Yue, D., Guo, S., Wiedensohler, A., and Wu, Z.: Estimation of size-resolved ambient
793   particle density based on the measurement of aerosol number, mass, and chemical size
794   distributions in the winter in Beijing, Environ. Sci. Technol., 120830075118007,
795   doi:10.1021/es204073t, 2012.

796 Huang, X.-F., He, L.-Y., Hu, M., Canagaratna, M. R., Sun, Y., Zhang, Q., Zhu, T., Xue, L., Zeng, L.-W., Liu, X.-
797   G., Zhang, Y.-H., Jayne, J. T., Ng, N. L., and Worsnop, D. R.: Highly time-resolved chemical
798   characterization of atmospheric submicron particles during 2008 Beijing Olympic Games using an
799   aerodyne high-resolution aerosol mass spectrometer, Atmos. Chem. Phys., 10(18), 8933–8945,
800   doi:10.5194/acp-10-8933-2010, 2010.

801 Janssen, S., Ewert, F., Li, H., Athanasiadis, I. N., Wien, J. J. F., Thérond, O., Knapen, M. J. R., Bezlepkina, I.,
802   Alkan-Olsson, J., Rizzoli, A. E., Belhouchette, H., Svensson, M., and van Ittersum, M. K.: Defining
803   assessment projects and scenarios for policy support: use of ontology in integrated assessment
804   and modelling, Environ. Modell. Softw., 24(12), 1491–1500, doi:10.1016/j.envsoft.2009.04.009,
805   2009.

806 Jayne, J. T., Leard, D. C., Zhang, X., Davidovits, P., Smith, K. A., Kolb, C. E., and Worsnop, D. R.: Development
807   of an aerosol mass spectrometer for size and composition analysis of submicron particles, Aerosol
808   Sci. Tech., 33(1-2), 49–70, 2000.

809 Jimenez, J. L., Canagaratna, M. R., Donahue, N. M., Prevot, A. S. H., Zhang, Q., Kroll, J. H., DeCarlo, P. F.,
810   Allan, J. D., Coe, H., Ng, N. L., Aiken, A. C., Docherty, K. S., Ulbrich, I. M., Grieshop, A. P., Robinson,
811   A. L., Duplissy, J., Smith, J. D., Wilson, K. R., Lanz, V. A., Hueglin, C., Sun, Y. L., Tian, J., Laaksonen,
812   A., Raatikainen, T., Rautiainen, J., Vaattovaara, P., Ehn, M., Kulmala, M., Tomlinson, J. M., Collins,
813   D. R., Cubison, M. J., Dunlea, J., Huffman, J. A., Onasch, T. B., Alfarra, M. R., Williams, P. I., Bower,
814   K., Kondo, Y., Schneider, J., Drewnick, F., Borrmann, S., Weimer, S., Demerjian, K., Salcedo, D.,
815   Cottrell, L., Griffin, R., Takami, A., Miyoshi, T., Hatakeyama, S., Shimono, A., Sun, J. Y., Zhang, Y.
816   M., Dzepina, K., Kimmel, J. R., Sueper, D., Jayne, J. T., Herndon, S. C., Trimborn, A. M., Williams, L.
817   R., Wood, E. C., Middlebrook, A. M., Kolb, C. E., Baltensperger, U., and Worsnop, D. R.: Evolution
818   of organic aerosols in the atmosphere, Science, 326(5959), 1525–1529,
819   doi:10.1126/science.1180353, 2009.

820 Kroll, J. H., Donahue, N. M., Jimenez, J. L., Kessler, S. H., Canagaratna, M. R., Wilson, K. R., Altieri, K. E.,
821   Mazzoleni, L. R., Wozniak, A. S., Bluhm, H., Mysak, E. R., Smith, J. D., Kolb, C. E., and Worsnop, D.
822   R.: Carbon oxidation state as a metric for describing the chemistry of atmospheric organic aerosol,
823   Nat. Chem., 3(2), 133–139, doi:10.1038/nchem.948, 2011.

824 Kukkonen, J., Pohjola, M., Ssokhi, R., Luhana, L., Kitwiroon, N., Fragkou, L., Rantamaki, M., Berge, E.,
825   Odegaard, V., and Havardslordal, L.: Analysis and evaluation of selected local-scale PM air
826   pollution episodes in four European cities: Helsinki, London, Milan and Oslo, Atmos. Environ.,
827   39(15), 2759–2773, doi:10.1016/j.atmosenv.2004.09.090, 2005.

828 Kundu, S., Kawamura, K., Andreae, T. W., Hoffer, A., and Andreae, M. O.: Molecular distributions of
829   dicarboxylic acids, ketocarboxylic acids and α-dicarbonyls in biomass burning aerosols:
830   implications for photochemical production and degradation in smoke layers, Atmos. Chem. Phys.,
831   10(5), 2209–2225, doi:10.5194/acp-10-2209-2010, 2010.

832 Lanz, V. A., Alfarra, M. R., Baltensperger, U., Buchmann, B., Hueglin, C., and Prévôt, A. S. H.: Source
833   apportionment of submicron organic aerosols at an urban site by factor analytical modelling of
834   aerosol mass spectra, Atmos. Chem. Phys., 7(6), 1503–1522, doi:10.5194/acp-7-1503-2007, 2007.

835 Lanz, V. A., Prévôt, A. S. H., Alfarra, M. R., Weimer, S., Mohr, C., DeCarlo, P. F., Gianini, M. F. D., Hueglin,
836   C., Schneider, J., Favez, O., D'Anna, B., George, C., and Baltensperger, U.: Characterization of
837   aerosol chemical composition with aerosol mass spectrometry in Central Europe: an overview,
838   Atmos. Chem. Phys., 10(21), 10453–10471, 2010.

839 Larsen, B. R., Gilardoni, S., Stenström, K., Niedzialek, J., Jimenez, J., and Belis, C. A.: Sources for PM air
840   pollution in the Po Plain, Italy: II. Probabilistic uncertainty characterization and sensitivity analysis
841   of secondary and primary sources, Atmos. Environ., 50, 203–213,
842   doi:10.1016/j.atmosenv.2011.12.038, 2012.

843 Larssen, S., Sluyter, R., and Helmis, C.: Criteria for EUROAIRNET, the EEA Air Quality Monitoring and
844   Information Network, available at:
845   http://www.eea.europa.eu/publications/TEC12/at_download/file (last access: 10 February
846   2016), 1999.

847 Lee, T., Sullivan, A. P., Mack, L., Jimenez, J. L., Kreidenweis, S. M., Onasch, T. B., Worsnop, D. R., Malm, W.,
848   Wold, C. E., Hao, W. M., and Collett, J. L.: Chemical smoke marker emissions during flaming and
849   smoldering phases of laboratory open burning of wildland fuels, Aerosol Sci. Tech., 44(9), i–v,
850   doi:10.1080/02786826.2010.499884, 2010.

851 Liu, P. S. K., Deng, R., Smith, K. A., Williams, L. R., Jayne, J. T., Canagaratna, M. R., Moore, K., Onasch, T. B.,
852   Worsnop, D. R., and Deshler, T.: Transmission efficiency of an aerodynamic focusing lens system:
853   comparison of model calculations and laboratory measurements for the Aerodyne aerosol mass
854   spectrometer, Aerosol Sci. Tech., 41(8), 721–733, doi:10.1080/02786820701422278, 2007.

855 Maimone, F., Turpin, B. J., Solomon, P., Meng, Q., Robinson, A. L., Subramanian, R., and Polidori, A.:
856   Correction methods for organic carbon artifacts when using quartz-fiber filters in large particulate
857   matter monitoring networks: the regression method and other options, J. Air Waste Manage.
858   Assoc., 61(6), 696–710, doi:10.3155/1047-3289.61.6.696, 2011.

859 McMurry, P. H., Wang, X., Park, K., and Ehara, K.: The relationship between mass and mobility for
860   atmospheric particles: a new technique for measuring particle density, Aerosol Sci. Tech., 36(2),
861   227–238, doi:10.1080/027868202753504083, 2002.

862 Middlebrook, A. M., Bahreini, R., Jimenez, J. L., and Canagaratna, M. R.: Evaluation of composition-
863   dependent collection efficiencies for the Aerodyne aerosol mass spectrometer using field data,
864   Aerosol Sci. Tech., 46(3), 258–271, doi:10.1080/02786826.2011.620041, 2012.

865 Miljevic, B., Heringa, M. F., Keller, A., Meyer, N. K., Good, J., Lauber, A., Decarlo, P. F., Fairfull-Smith, K. E.,
866   Nussbaumer, T., Burtscher, H., Prévôt, A. S. H., Baltensperger, U., Bottle, S. E., and Ristovski, Z. D.:
867   Oxidative potential of logwood and pellet burning particles assessed by a novel profluorescent
868   nitroxide probe, Environ. Sci. Technol., 44(17), 6601–6607, 2010.

869 Minguillón, M. C., Ripoll, A., Pérez, N., Prévôt, A. S. H., Canonaco, F., Querol, X., and Alastuey, A.: Chemical
870   characterization of submicron regional background aerosols in the western Mediterranean using
871   an aerosol chemical speciation monitor, Atmos. Chem. Phys., 15(11), 6379–6391,
872   doi:10.5194/acp-15-6379-2015, 2015.

873 Naeher, L. P., Brauer, M., Lipsett, M., Zelikoff, J. T., Simpson, C. D., Koenig, J. Q., and Smith, K. R.:
874   Woodsmoke health effects: a review, Inhal. Toxicol., 19(1), 67–106,
875   doi:10.1080/08958370600985875, 2007.

876 Ng, N. L., Herndon, S. C., Trimborn, A., Canagaratna, M. R., Croteau, P. L., Onasch, T. B., Sueper, D.,
877   Worsnop, D. R., Zhang, Q., Sun, Y. L., and Jayne, J. T.: An aerosol chemical speciation monitor
878   (ACSM) for routine monitoring of the composition and mass concentrations of ambient aerosol,
879   Aerosol Sci. Tech., 45(7), 780–794, doi:10.1080/02786826.2011.560211, 2011a.

880 Ng, N. L., Canagaratna, M. R., Jimenez, J. L., Chhabra, P. S., Seinfeld, J. H., and Worsnop, D. R.: Changes in
881   organic aerosol composition with aging inferred from aerosol mass spectra, Atmos. Chem. Phys.,
882   11(13), 6465–6474, doi:10.5194/acp-11-6465-2011, 2011b.
883 Ng, N. L., Canagaratna, M. R., Jimenez, J. L., Zhang, Q., Ulbrich, I. M., and Worsnop, D. R.: Real-time
884   methods for estimating organic component mass concentrations from aerosol mass spectrometer
885   data, Environ. Sci. Technol., 45(3), 910–916, doi:10.1021/es102951k, 2011c.
886 Paatero, P.: User's guide for the multilinear engine program "ME2" for fitting multilinear and
887   quasimultilinear models, University of Helsinki, Finland, 2000.
888 Paatero, P. and Tapper, U.: Positive matrix factorization - a nonnegative factor model with optimal
889   utilization of error-estimates of data values, Environmetrics, 5(2), 111–126,
890   doi:10.1002/env.3170050203, 1994.
891 Paglione, M., Saarikoski, S., Carbone, S., Hillamo, R., Facchini, M. C., Finessi, E., Giulianelli, L., Carbone, C.,
892   Fuzzi, S., Moretti, F., Tagliavini, E., Swietlicki, E., Eriksson Stenström, K., Prévôt, A. S. H., Massoli,
893   P., Canaragatna, M., Worsnop, D., and Decesari, S.: Primary and secondary biomass burning
894   aerosols determined by proton nuclear magnetic resonance (^{1}H-NMR) spectroscopy during the
895   2008 EUCAARI campaign in the Po Valley (Italy), Atmos. Chem. Phys., 14(10), 5089–5110,
896   doi:10.5194/acp-14-5089-2014, 2014.
897 Pernigotti, D., Georgieva, E., Thunis, P., and Bessagnet, B.: Impact of meteorology on air quality modeling
898   over the Po valley in northern Italy, Atmos. Environ., 51, 303–310,
899   doi:10.1016/j.atmosenv.2011.12.059, 2012.
900 Perrone, M. G., Larsen, B. R., Ferrero, L., Sangiorgi, G., De Gennaro, G., Udisti, R., Zangrando, R., Gambaro,
901   A., and Bolzacchini, E.: Sources of high $PM_{2.5}$ concentrations in Milan, northern Italy: molecular
902   marker data and CMB modelling, Sci. Total Environ., 414, 343–355,
903   doi:10.1016/j.scitotenv.2011.11.026, 2012.
904 Petit, J.-E., Favez, O., Sciare, J., Crenn, V., Sarda-Estève, R., Bonnaire, N., Močnik, G., Dupont, J.-C.,
905   Haeffelin, M., and Leoz-Garziandia, E.: Two years of near real-time chemical composition of
906   submicron aerosols in the region of Paris using an aerosol chemical speciation monitor (ACSM)
907   and a multi-wavelength aethalometer, Atmos. Chem. Phys., 15, 2985–3005, doi:10.5194/acp-15-
908   2985-2015, 2015.
909 Pitz, M., Cyrys, J., Karg, E., Wiedensohler, A., Wichmann, H.-E., and Heinrich, J.: Variability of apparent
910   particle density of an urban aerosol, Environ. Sci. Technol., 37(19), 4336–4342,
911   doi:10.1021/es034322p, 2003.
912 Pitz, M., Schmid, O., Heinrich, J., Birmili, W., Maguhn, J., Zimmermann, R., Wichmann, H.-E., Peters, A.,
913   and Cyrys, J.: Seasonal and diurnal variation of $PM_{2.5}$ apparent particle density in urban air in
914   Augsburg, Germany, Environ. Sci. Technol., 42(14), 5087–5093, 2008.
915 Putaud, J. P., Van Dingenen, R., and Raes, F.: Submicron aerosol mass balance at urban and semirural sites
916   in the Milan area (Italy), J. Geophys. Res.-Atmos., 107(D22), LOP 11–1–LOP 11–10,
917   doi:10.1029/2000JD000111, 2002.
918 Putaud, J.-P., Van Dingenen, R., Alastuey, A., Bauer, H., Birmili, W., Cyrys, J., Flentje, H., Fuzzi, S., Gehrig,
919   R., Hansson, H. C., Harrison, R. M., Herrmann, H., Hitzenberger, R., Huglin, C., Jones, A. M., Kasper-
920   Giebl, A., Kiss, G., Kousa, A., Kuhlbusch, T. A. J., Loschau, G., Maenhaut, W., Molnar, A., Moreno,
921   T., Pekkanen, J., Perrino, C., Pitz, M., Puxbaum, H., Querol, X., Rodriguez, S., Salma, I., Schwarz, J.,
922   Smolik, J., Schneider, J., Spindler, G., ten Brink, H., Tursic, J., Viana, M., Wiedensohler, A., and
923   Raes, F.: A European aerosol phenomenology – 3: physical and chemical characteristics of
924   particulate matter from 60 rural, urban, and kerbside sites across Europe, Atmos. Environ., 44,
925   1308–1320, 2010.
926 Putaud, J.-P., Adam, M., Belis, C. A., Bergamaschi, P., Cancellinha, J., Cavalli, F., Cescatti, A., Daou, D.,
927   Dell'Acqua, A., Douglas, K., Duerr, M., Goded, I., Grassi, F., Gruening, C., Hjorth, J., Jensen, N. R.,

928   Lagler, F., Manca, G., Martins Dos Santos, S., Passarella, R., Pedroni, V., Rocha e Abreu, P., Roux,
929   D., Scheeren, B., and Schembari, C.: JRC-Ispra Atmosphere-Biosphere-Climate Integrated
930   monitoring Station (ABC-IS): 2011 report, JRC Technical Reports, Joint Research Centre, Ispra
931   (Italy),   available   at:
932   http://publications.jrc.ec.europa.eu/repository/bitstream/111111111/28242/1/lb-na-25753-en-
933   n.pdf (last access: 28 March 2014), 2013.
934   Putaud, J.-P., Bergamaschi, P., Bressi, M., Cavalli, F., Cescatti, A., Daou, D., Dell'acqua, A., Douglas, K.,
935   Duerr, M., Fumagalli, I., Goded Ballarin, I., Grassi, F., Gruening, C., Hjorth, J., Jensen, N., Lagler, F.,
936   Manca, G., Martins Dos Santos, S., Matteucci, M., Passarella, R., Pedroni, V., Pokorska, O., and
937   Roux, D.: JRC – Ispra Atmosphere – Biosphere – Climate Integrated monitoring Station 2013
938   report, EUR - Scientific and Technical Research Reports, Publications Office of the European
939   Union, available at: http://publications.jrc.ec.europa.eu/repository/handle/111111111/33904
940   (last access: 19 February 2015), 2014a.
941   Putaud, J. P., Cavalli, F., Martins dos Santos, S., and Dell'Acqua, A.: Long-term trends in aerosol optical
942   characteristics in the Po Valley, Italy, Atmos. Chem. Phys., 14(17), 9129–9136, doi:10.5194/acp-
943   14-9129-2014, 2014b.
944   Reiss, R., Anderson, E. L., Cross, C. E., Hidy, G., Hoel, D., McClellan, R., and Moolgavkar, S.: Evidence of
945   health impacts of sulfate- and nitrate-containing particles in ambient air, Inhal. Toxicol., 19(5),
946   419–449, doi:10.1080/08958370601174941, 2007.
947   Riffault, V., Zhang, S., Tison, E., and Setyan, A.: Chloride RIE measurements, 14th AMS user meeting, 8
948   September   2013,   available   at: http://cires.colorado.edu/jimenez-
949   group/UsrMtgs/UsersMtg14/AMS_user_meeting_Chl_RIE_riffault.pdf (last access: 10 February
950   2016), 2013.
951   Ripoll, A., Minguillón, M. C., Pey, J., Jimenez, J. L., Day, D. A., Sosedova, Y., Canonaco, F., Prévôt, A. S. H.,
952   Querol, X., and Alastuey, A.: Long-term real-time chemical characterization of submicron aerosols
953   at Montsec (southern Pyrenees, 1570 m a.s.l.), Atmos. Chem. Phys., 15(6), 2935–2951,
954   doi:10.5194/acp-15-2935-2015, 2015.
955   Saarikoski, S., Carbone, S., Decesari, S., Giulianelli, L., Angelini, F., Canagaratna, M., Ng, N. L., Trimborn, A.,
956   Facchini, M. C., Fuzzi, S., Hillamo, R., and Worsnop, D.: Chemical characterization of springtime
957   submicrometer aerosol in Po Valley, Italy, Atmos. Chem. Phys., 12(18), 8401–8421,
958   doi:10.5194/acp-12-8401-2012, 2012.
959   Schaap, M., Van Loon, M., Ten Brink, H. M., Dentener, F. J., and Builtjes, P. J. H.: Secondary inorganic
960   aerosol simulations for Europe with special attention to nitrate, Atmos. Chem. Phys., 4(3), 857–
961   874, 2004.
962   Schlesinger, R. B. and Cassee, F.: Atmospheric secondary inorganic particulate matter: the toxicological
963   perspective as a basis for health effects risk assessment, Inhal. Toxicol., 15(3), 197–235,
964   doi:10.1080/08958370390168247, 2003.
965   Seinfeld, J. H. and Pandis, S. N.: Atmospheric Chemistry and Physics: from Air Pollution to Climate Change,
966   Wiley, New York, USA, 2006.
967   Sturtz, T. M., Adar, S. D., Gould, T., and Larson, T. V.: Constrained source apportionment of coarse
968   particulate matter and selected trace elements in three cities from the multi-ethnic study of
969   atherosclerosis, Atmos. Environ., 84, 65–77, doi:10.1016/j.atmosenv.2013.11.031, 2014.
970   Sun, Y., Wang, Z., Dong, H., Yang, T., Li, J., Pan, X., Chen, P., and Jayne, J. T.: Characterization of summer
971   organic and inorganic aerosols in Beijing, China with an aerosol chemical speciation monitor,
972   Atmos. Environ., 51, 250–259, doi:10.1016/j.atmosenv.2012.01.013, 2012.
973   Takegawa, N., Miyazaki, Y., Kondo, Y., Komazaki, Y., Miyakawa, T., Jimenez, J. L., Jayne, J. T., Worsnop, D.
974   R., Allan, J. D., and Weber, R. J.: Characterization of an Aerodyne aerosol mass spectrometer

975   (AMS): intercomparison with other aerosol instruments, Aerosol Sci. Tech., 39(8), 760–770,
976   doi:10.1080/02786820500243404, 2005.
977 Takegawa, N., Miyakawa, T., Kondo, Y., Jimenez, J. L., Zhang, Q., Worsnop, D. R., and Fukuda, M.: Seasonal
978   and diurnal variations of submicron organic aerosol in Tokyo observed using the Aerodyne aerosol
979   mass spectrometer, J. Geophys. Res.-Atmos., 111(D11), D11206, doi:10.1029/2005JD006515,
980   2006.
981 Turpin, B. J. and Lim, H. J.: Species contributions to $PM_{2.5}$ mass concentrations: revisiting common
982   assumptions for estimating organic mass, Aerosol Sci. Tech., 35(1), 602–610,
983   doi:10.1080/02786820152051454, 2001.
984 Turpin, B. J., Saxena, P., and Andrews, E.: Measuring and simulating particulate organics in the
985   atmosphere: problems and prospects, Atmos. Environ., 34(18), 2983–3013, 2000.
986 Ulbrich, I. M., Canagaratna, M. R., Zhang, Q., Worsnop, D. R., and Jimenez, J. L.: Interpretation of organic
987   components from positive matrix factorization of aerosol mass spectrometric data, Atmos. Chem.
988   Phys., 9(9), 2891–2918, 2009.
989 Ulbrich, I. M., Lechner, M., and Jimenez, J. L.: AMS Spectral Database, available at:
990   http://cires.colorado.edu/jimenez-group/AMSsd/ (last access: 7 October 2015), 2015.
991 van Donkelaar, A., Martin, R. V., Brauer, M., Kahn, R., Levy, R., Verduzco, C., and Villeneuve, P. J.: Global
992   estimates of ambient fine particulate matter concentrations from satellite-based aerosol optical
993   depth: development and application, Environ. Health Persp., 118(6), 847–855,
994   doi:10.1289/ehp.0901623, 2010.
995 Volkamer, R., Jimenez, J. L., San Martini, F., Dzepina, K., Zhang, Q., Salcedo, D., Molina, L. T., Worsnop, D.
996   R., and Molina, M. J.: Secondary organic aerosol formation from anthropogenic air pollution: rapid
997   and higher than expected, Geophys. Res. Lett., 33(17), doi:10.1029/2006GL026899, 2006.
998 Watson, J. G., Chow, J. C., Chen, L.-W. A., and Frank, N. H.: Methods to assess carbonaceous aerosol
999   sampling artifacts for IMPROVE and other long-term networks, J. Air Waste Manage. Assoc., 59(8),
1000   898–911, doi:10.3155/1047-3289.59.8.898, 2009.
1001 Weimer, S., Drewnick, F., Hogrefe, O., Schwab, J. J., Rhoads, K., Orsini, D., Canagaratna, M., Worsnop, D.
1002   R., and Demerjian, K. L.: Size-selective nonrefractory ambient aerosol measurements during the
1003   particulate matter technology assessment and characterization study - New York 2004 winter
1004   intensive in New York City, J. Geophys. Res., 111(D18), doi:10.1029/2006JD007215, 2006.
1005 WHO: WHO Air quality guidelines for particulate matter, ozone, nitrogen dioxide and sulfur dioxide: global
1006   update 2005: summary of risk assessment, available at:
1007   http://apps.who.int/iris/handle/10665/69477 (last access: 10 October 2014), 2006.
1008 WHO: Review of evidence on health aspects of air pollution_ REVIHAAP Project, Technical Report,
1009   available at: http://www.euro.who.int/__data/assets/pdf_file/0004/193108/REVIHAAP-Final-
1010   technical-report-final-version.pdf (last access: 15 April 2015), 2013.
1011 Wiedensohler, A., Birmili, W., Nowak, A., Sonntag, A., Weinhold, K., Merkel, M., Wehner, B., Tuch, T.,
1012   Pfeifer, S., Fiebig, M., Fjäraa, A. M., Asmi, E., Sellegri, K., Depuy, R., Venzac, H., Villani, P., Laj, P.,
1013   Aalto, P., Ogren, J. A., Swietlicki, E., Williams, P., Roldin, P., Quincey, P., Hüglin, C., Fierz-
1014   Schmidhauser, R., Gysel, M., Weingartner, E., Riccobono, F., Santos, S., Grüning, C., Faloon, K.,
1015   Beddows, D., Harrison, R., Monahan, C., Jennings, S. G., O'Dowd, C. D., Marinoni, A., Horn, H.-G.,
1016   Keck, L., Jiang, J., Scheckman, J., McMurry, P. H., Deng, Z., Zhao, C. S., Moerman, M., Henzing, B.,
1017   de Leeuw, G., Löschau, G., and Bastian, S.: Mobility particle size spectrometers: harmonization of
1018   technical standards and data structure to facilitate high quality long-term observations of
1019   atmospheric particle number size distributions, Atmos. Meas. Tech., 5(3), 657–685,
1020   doi:10.5194/amt-5-657-2012, 2012.
1021 WMO, Zhu, T., Melamed, M., Parrish, D., Gauss, M., Gallardo Klenner, L., Lawrence, M., Konare, A., and
1022   Liousse, C.: WMO/IGAC impacts of megacities on air pollution and climate, available at:

1023 http://www.igacproject.org/sites/all/themes/bluemasters/images/GAW Report 205.pdf (last
1024 access: 29 July 2015), 2012.
1025 Young, D. E., Allan, J. D., Williams, P. I., Green, D. C., Harrison, R. M., Yin, J., Flynn, M. J., Gallagher, M. W.,
1026 and Coe, H.: Investigating a two-component model of solid fuel organic aerosol in London:
1027 processes, PM$_1$ contributions, and seasonality, Atmos. Chem. Phys., 15(5), 2429–2443,
1028 doi:10.5194/acp-15-2429-2015, 2015.
1029 Zhang, Q.: Time- and size-resolved chemical composition of submicron particles in Pittsburgh: implications
1030 for aerosol sources and processes, J. Geophys. Res., 110(D7), doi:10.1029/2004JD004649, 2005.
1031 Zhang, Q., Jimenez, J. L., Canagaratna, M. R., Allan, J. D., Coe, H., Ulbrich, I., Alfarra, M. R., Takami, A.,
1032 Middlebrook, A. M., Sun, Y. L., Dzepina, K., Dunlea, E., Docherty, K., DeCarlo, P. F., Salcedo, D.,
1033 Onasch, T., Jayne, J. T., Miyoshi, T., Shimono, A., Hatakeyama, S., Takegawa, N., Kondo, Y.,
1034 Schneider, J., Drewnick, F., Borrmann, S., Weimer, S., Demerjian, K., Williams, P., Bower, K.,
1035 Bahreini, R., Cottrell, L., Griffin, R. J., Rautiainen, J., Sun, J. Y., Zhang, Y. M., and Worsnop, D. R.:
1036 Ubiquity and dominance of oxygenated species in organic aerosols in anthropogenically-
1037 influenced Northern Hemisphere midlatitudes, Geophys. Res. Lett., 34(13),
1038 doi:10.1029/2007GL029979, 2007.
1039 Zhang, Q., Jimenez, J. L., Canagaratna, M. R., Ulbrich, I. M., Ng, N. L., Worsnop, D. R., and Sun, Y.:
1040 Understanding atmospheric organic aerosols via factor analysis of aerosol mass spectrometry: a
1041 review, Anal. Bioanal. Chem., 401(10), 3045–3067, doi:10.1007/s00216-011-5355-y, 2011.

1042   **Tables and Figures**

1043

1044   Table 1. Consistency of ACSM measurements: comparison between ACSM and independent analytical techniques using orthogonal regression

1045   analyses. Slopes and intercepts are indicated ± uncertainties.

1046

	r^2					slope					intercept				
	Sp	Su	Au	Wi	An	Sp	Su	Au	Wi	An	Sp	Su	Au	Wi	An
Org vs OC	0.91	0.90	0.86	0.92	0.77	2.18 ± 0.07	2.92 ± 0.10	1.87 ± 0.09	1.26 ± 0.04	1.72 ± 0.04	-0.29 ± 0.37	-1.07 ± 0.32	-0.28 ± 0.36	0.74 ± 0.37	0.61 ± 0.25
Nitrate	0.95	0.53	0.96	0.92	0.91	1.37 ± 0.03	4.27 ± 0.25	1.28 ± 0.03	0.86 ± 0.03	1.28 ± 0.02	0.42 ± 0.18	0.64 ± 0.11	0.48 ± 0.10	0.62 ± 0.11	0.48 ± 0.09
Sulfate	0.96	0.97	0.92	0.86	0.95	1.05 ± 0.02	0.98 ± 0.02	0.96 ± 0.04	1.38 ± 0.06	1.00 ± 0.01	-0.01 ± 0.04	0.02 ± 0.06	0.04 ± 0.07	-0.25 ± 0.06	0.00 ± 0.03
Ammonium	0.92	0.70	0.91	0.95	0.90	1.03 ± 0.03	1.00 ± 0.06	0.93 ± 0.04	0.81 ± 0.02	0.99 ± 0.02	-0.04 ± 0.07	-0.04 ± 0.07	-0.12 ± 0.05	0.03 ± 0.03	-0.08 ± 0.03
Chloride	0.75	0.00	0.59	0.78	0.52	2.68 ± 0.13	-0.13 ± 0.09	0.68 ± 0.06	1.13 ± 0.07	1.75 ± 0.06	0.04 ± 0.01	0.03 ± 0.00	0.04 ± 0.00	-0.02 ± 0.01	0.02 ± 0.01
Mass vs volume	0.87	0.82	0.88	0.85	0.81	1.91 ± 0.01	1.95 ± 0.02	1.45 ± 0.01	1.34 ± 0.01	1.63 ± 0.01	-1.16 ± 0.19	-1.36 ± 0.18	-2.45 ± 0.19	-0.11 ± 0.20	-1.09 ± 0.11

1047

1048

1049   Legend: Sp: spring (March-April-May), Su: summer (June-July-August), Au: autumn (September-October-November), Wi: winter (December-

1050   January-February), An: annual. Independent analytical techniques refer to i) EC-OC Sunset Analyzer for OC from $PM_{2.5}$ sampling, ii) Ion

1051   Chromatography for ions from $PM_{2.5}$ sampling and iii) DMPS for volume concentrations (see Sect. 2.3 for more details). Mass refers to NR-PM_1+BC.

1052   Intercepts are in µg/m^3. Slopes are in g/cm^3 for mass vs volume and dimensionless otherwise.

1053   Table 2. Comparison (coefficient of determination, r^2) between SA factors, organic m/z tracers and independent species time series. BC stands

1054   for Black Carbon; Org_i stands for organic signal at m/z i (i=43, 44, 60, 67, 73, 81).

1055

		HOA					BBOA					OOA			
		Org_67	Org_81	NOx	CO	BC	Org_60	Org_73	NOx	CO	BC	Org_43	Org_44	NH4	SO4	NO3
	SPRING	0.60	0.55	0.03	0.08	0.28	0.99	0.97	0.32	0.81	0.70	0.88	0.94	0.76	0.43	0.77
	SUMMER	0.90	0.91	0.07	0.40	0.52			-			0.97	0.94	0.54	0.60	0.19
	AUTUMN	0.63	0.61	0.07	0.10	0.24	0.99	0.97	0.06	0.68	0.47	0.82	0.92	0.47	0.53	0.38
	WINTER	0.58	0.57	0.34	0.33	0.39	0.98	0.97	0.20	0.66	0.63	0.80	0.99	0.50	0.39	0.66

1056

1057
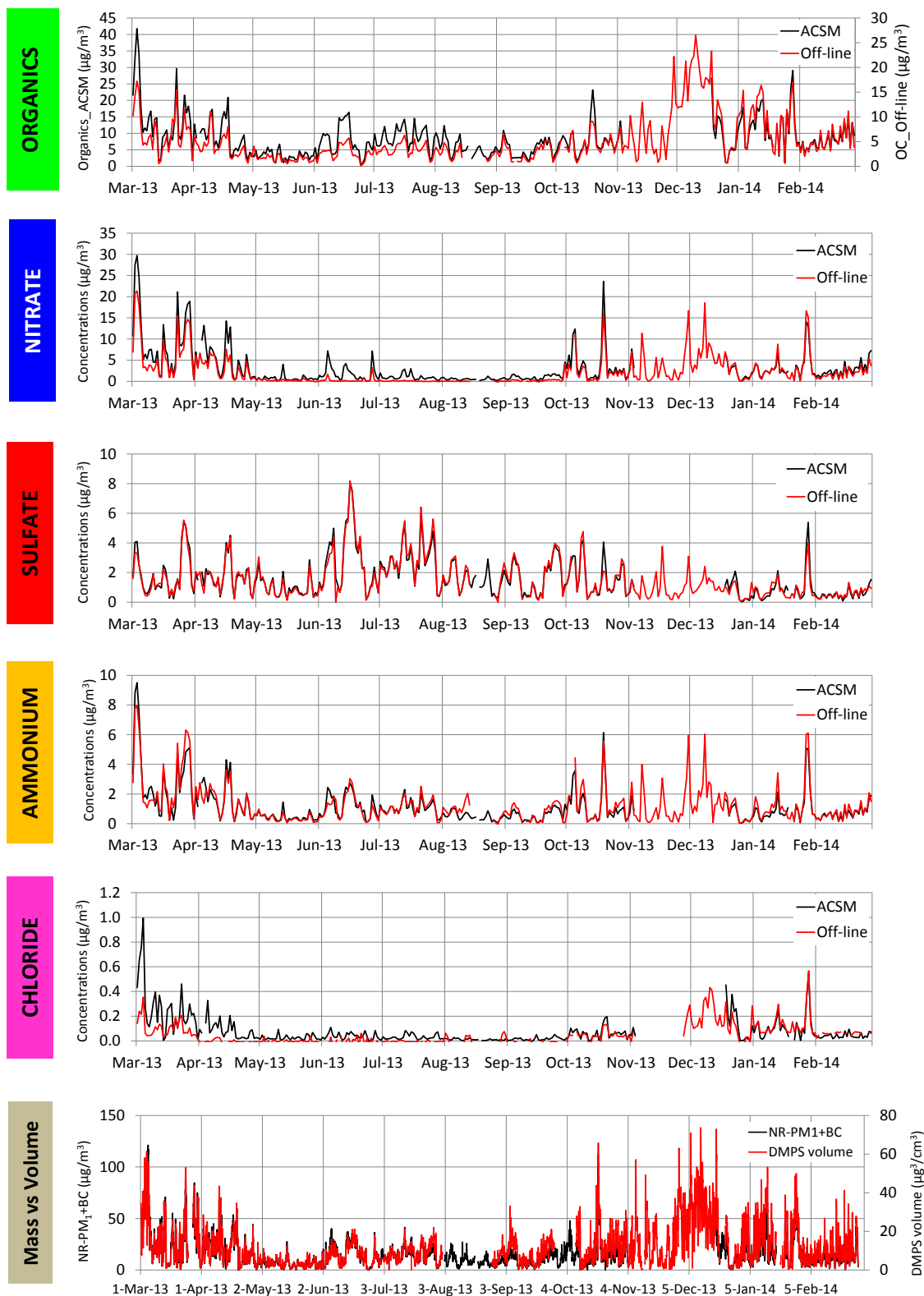
1058   Figure 1. Comparison between measurements performed with the ACSM and other co-located analytical

1059   techniques. See Table 1 and Sect. 2.3 for more details.

1060
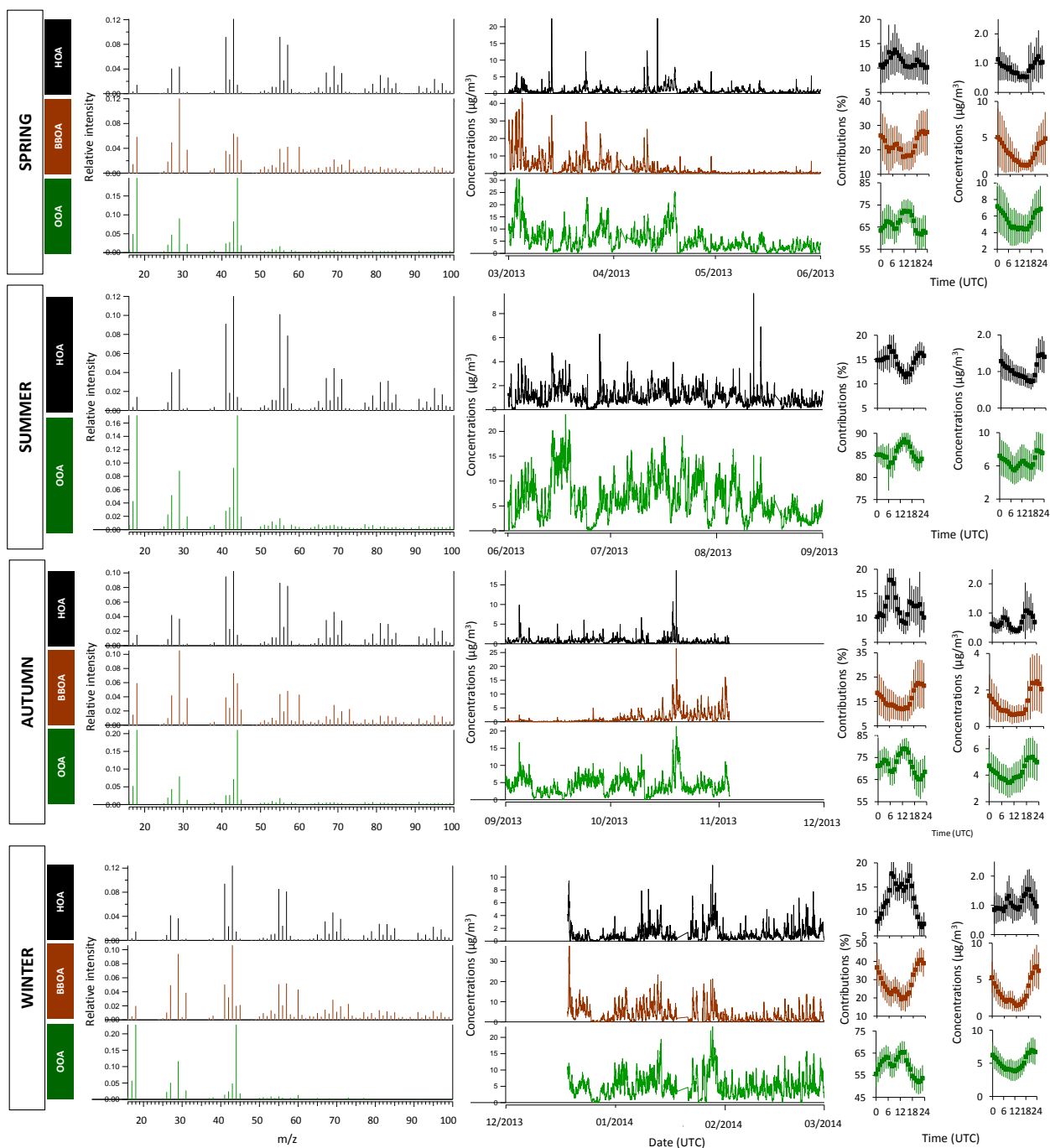
1061   Figure 2. Organic source apportionment presented by season: factor profiles (left), time series (middle)

1062   and daily cycles (right, error bars represent 1 standard deviation). Seasons are defined as Spring: MAM,

1063   Summer: JJA, Autumn: SON and Winter: DJF.
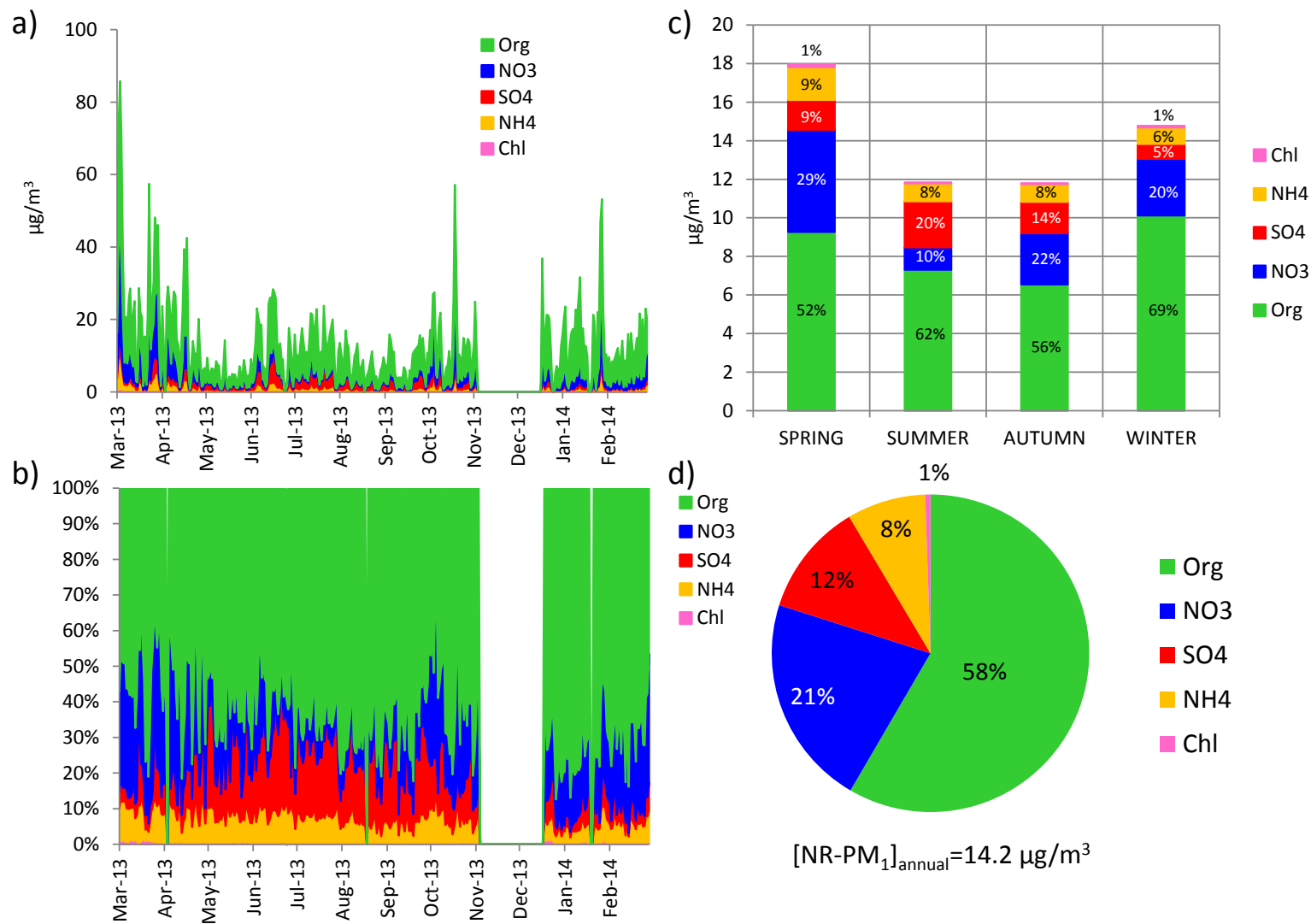
1064

1065   Figure 3. Overview of the chemical composition of NR-PM$_1$ at Ispra (Po Valley, Italy): daily absolute (a) and relative (b) chemical composition;

1066   seasonal (c) and annual (d) averages.
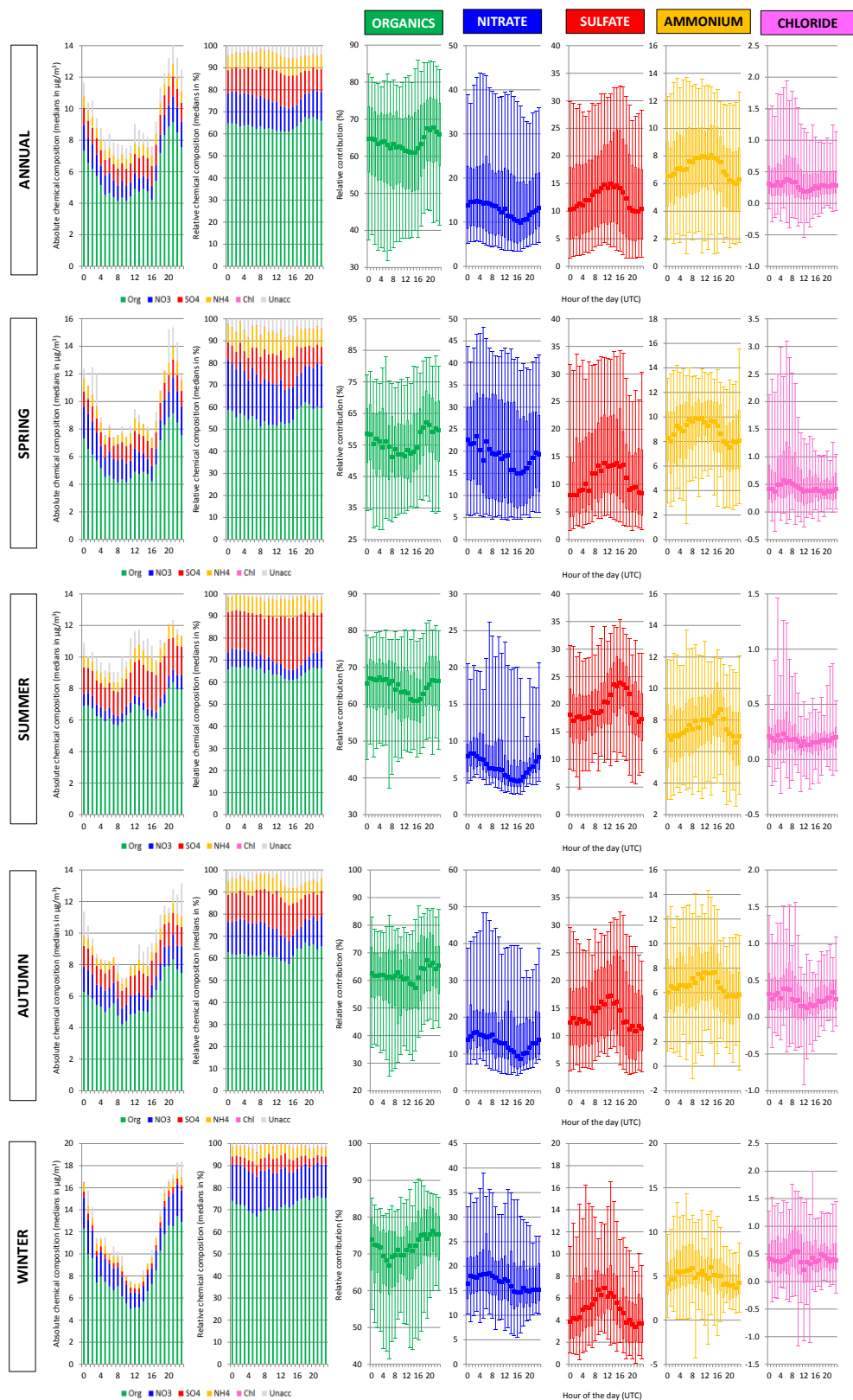
1067

Figure 4. Daily cycles of NR-PM$_1$ chemical composition on the annual and seasonal scales. Unacc: unaccounted mass, whisker plots are constructed from the 5th, 25th, 50th, 75th and 95th percentiles.
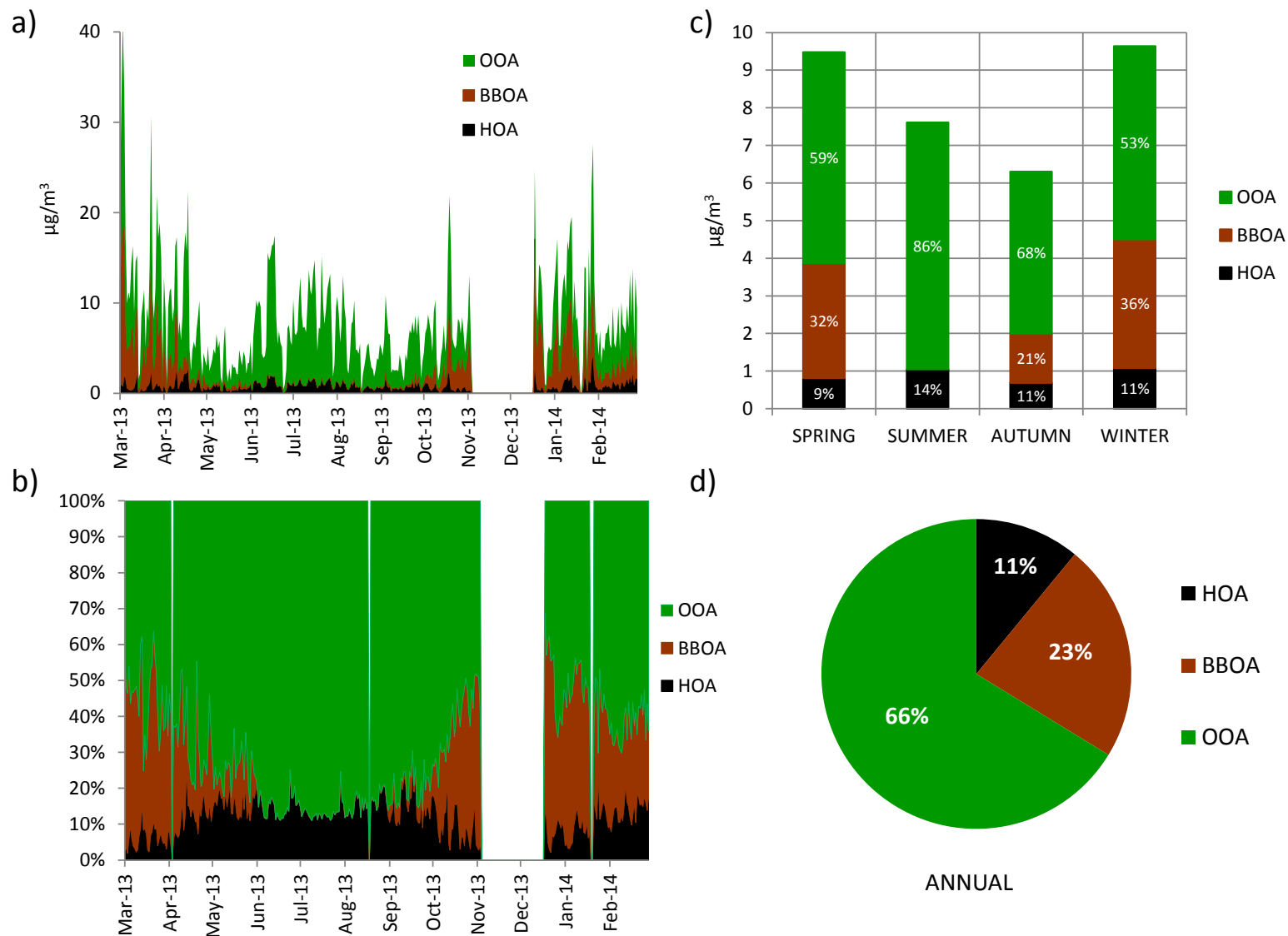
1070

1071   Figure 5. Overview of HOA, BBOA and OOA contributions to organic aerosols; see legend Figure 3.
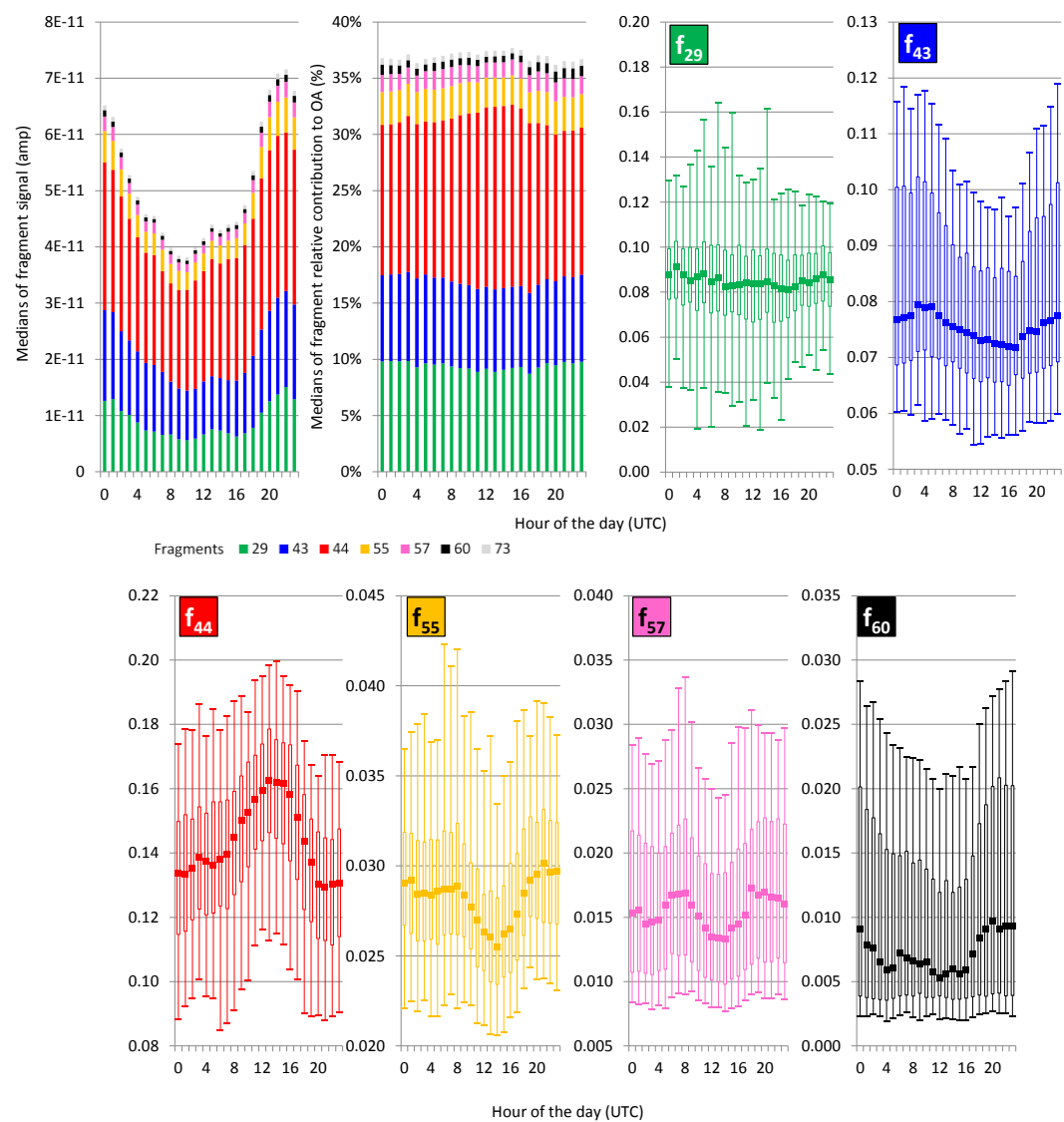
1072

1073   Figure 6. Annual statistics describing the daily cycles of the major organic fragments. Box plots are constructed from the 5th, 25th, 50th, 75th and

1074   95th percentiles.
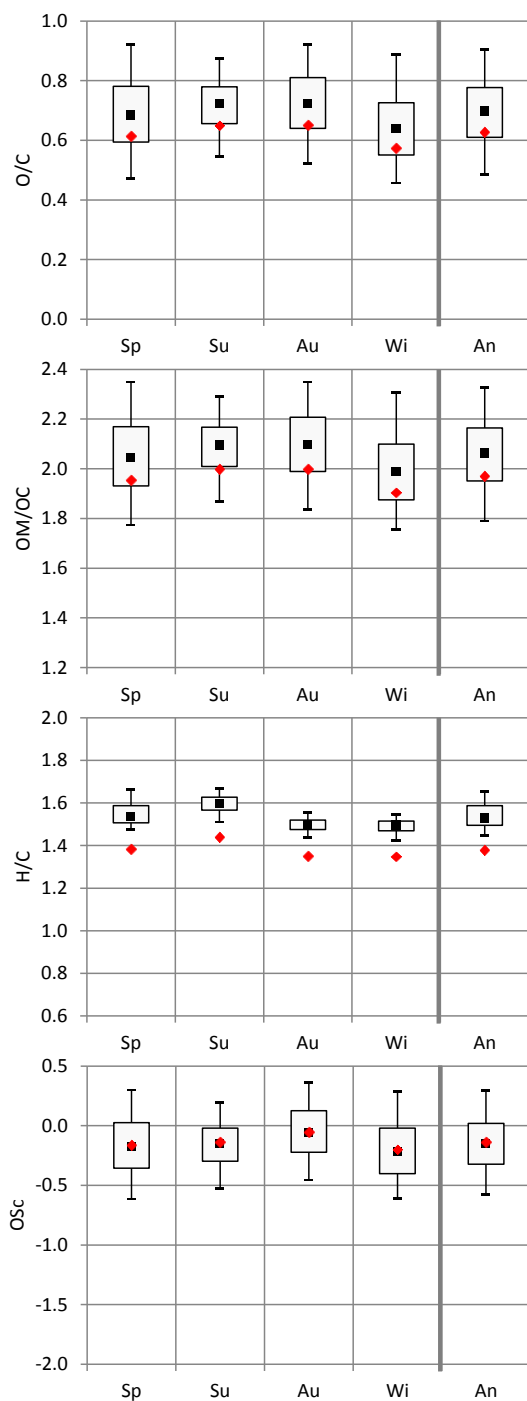
1075

Figure 7. Seasonal and annual O/C, OM/OC, H/C and OSc of ambient OA. Sp: spring (MAM), Su: summer (JJA), Au: autumn (SON), Wi: winter (DJF), An: annual. Black: 5th, 25th, 50th, 75th and 95th percentiles estimates following Canagaratna et al. (2015); red: median estimates following Aiken et al. (2008) for O/C and OM/C, Ng et al. (2011b) for H/C and Aiken et al. (2008), Kroll et al. (2011) and Ng et al. (2011b) for OSc. Note that the authors do not recommend comparing absolute O/C, OM/OC and OSc values reported here with other AMS studies, given the uncertainties associated with f_{44} quantifications from ACSM measurements (please see text).
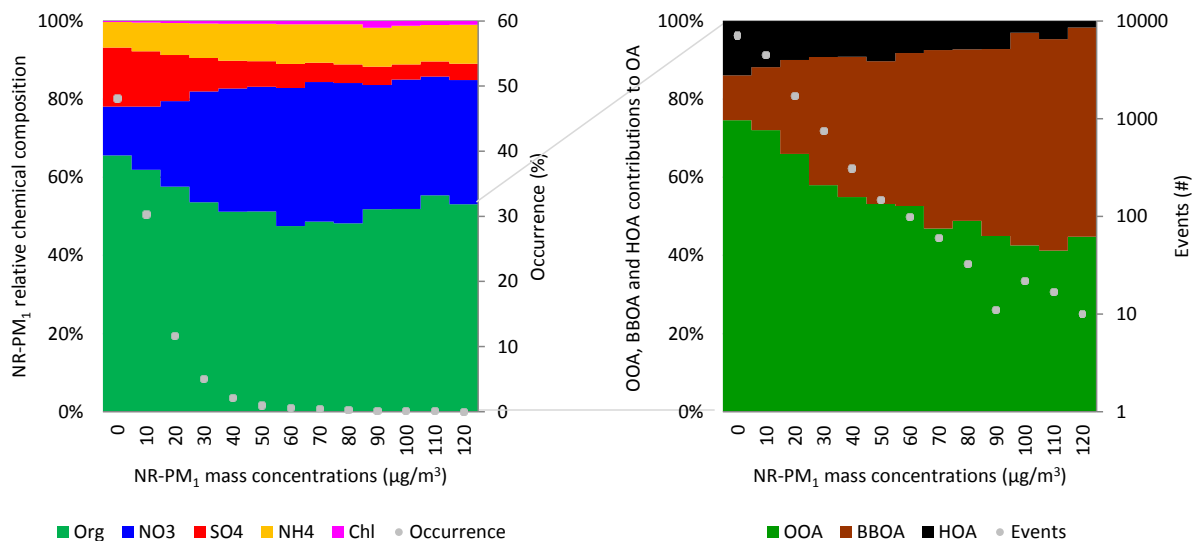
1083

Figure 8. NR-PM$_1$ relative chemical composition (left) and OA factor contributions (right) averages as a function of NR-PM$_1$ mass concentrations (bins of 10 µg/m^3). Occurrence (%, left) and number of pollution events (#, right) are indicated (solid dots) for each NR-PM$_1$ bin. Note that one event corresponds to one 30 minute average.